Entanglement properties of random quantum operators and effect of local dynamics

A Thesis

submitted to

Indian Institute of Science Education and Research Pune
in partial fulfillment of the requirements for the
BS-MS Dual Degree Programme

by

Namitha Pradeep

IISER PUNE

Indian Institute of Science Education and Research Pune
Dr. Homi Bhabha Road,
Pashan, Pune 411008, INDIA.

May, 2019

Supervisor: Dr.Prabha Mandayam
© Namitha Pradeep 2019

Certificate

This is to certify that this dissertation entitled Entanglement properties of random quantum operators and effect of local dynamics towards the partial fulfilment of the BS-MS dual degree programme at the Indian Institute of Science Education and Research, Pune represents study/work carried out by Namitha Pradeep at Indian Institute of Technology Madras under the supervision of Dr.Prabha Mandayam, Assistant Professor, Department of Physics, during the academic year 2018-2019.

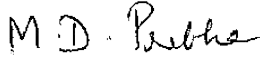Dr.Prabha Mandayam

Namitha Pradeep

Committee:

Dr.Prabha Mandayam

Dr. T.S.Mahesh

This thesis is dedicated to my parents

Declaration

I hereby declare that the matter embodied in the report entitled Entanglement properties of random quantum operators and effect of local dynamics are the results of the work carried out by me at the Department of Physics, Indian Institute of Technology Madras, under the supervision of Dr.Prabha Mandayam and the same has not been submitted elsewhere for any other degree.

Namitha Pradeep

Dr.Prabha Mandayam

Acknowledgments

Firstly, I would like to thank from the bottom of my heart, my supervisor Dr.Prabha Mandayam, for her continuous motivation and support. She is truly an inspiration and every single conversation with her was a great learning experience for me. I would also like to sincerely thank Dr.Arul Lakshminarayan for his valuable inputs. I express my deepest gratitude to Dr.T.S.Mahesh for being an amazing mentor over the last three years. He helped me build the foundations required for good research and he has been a source of constant support throughout my journey.

I would also like to thank IIT Madras for providing me with all the facilities. Last, but never the least, I convey my love and gratitude to my parents and all my friends for always being by my side.

x

Abstract

In this work, the ensemble of iterated unitary quantum gates distributed uniformly with respect to the Haar measure on the unitary group is studied. Instead of using random quantum circuits with non-local random unitaries, we look at what happens when there are fixed nonlocal unitaries but haar random locals at intermediate steps. Recently it was shown for a 2 qubit system that such an interlacing of local gates can lead to exponential growth of entanglement in time. Here we try to extend those results to a 4 qubit case.

We use the quantities *entangling power* (e_p) and *gate typicality* (g_t) to study the entangling properties of unitaries. We have done the study of 4 qubit case in two parts:

　　1.Firstly, we look at what set of gates form the boundaries of the $e_p - g_t$ phase space of $U(16)$. We try to anaytically derive these bounds on e_p and g_t as well.

　　2.The second part is mainly studying the phase space diagrams. We choose random unitary gates according to haar measure and see how the phase space changes with different combinations of local and nonlocal gates.

Contents

List of Figures

Chapter 1

Introduction

1.1 Entanglement - What and Why ?

Quantum entanglement is a key resource for several quantum information processing tasks. It is defined as the quantum mechanical phenomenon involving two or more objects, where the quantum state of each object cannot be described independently of the states of all others [1]. A pure state $|\psi>$ in a composite Hilbert space $\mathscr{H} = \mathscr{H}^A \otimes \mathscr{H}^B$, is unentangled if it can be written in product form i.e

$$|\psi> = |\psi>^A \otimes |\psi>^B$$

otherwise, it is entangled. Quantum entanglement is an integral part of many quantum computing tasks and quantum cryptography protocols. It has also been used to realize super dense coding and quantum teleportation. Hence, efficient generation of entanglement is an important area of study.

1.2 Why random unitaries and local gates ?

Random quantum circuits are useful in studying generic systems i.e, the dynamics of a random quantum circuit will help in understanding a generic Hamiltonian system. [2] Circuits with random unitary operators are also used as toy models for information scrambling in black holes and other strongly coupled systems. Other uses of random unitaries include approximate encryption of quantum information, quantum data hiding,information locking etc.

Recently it has been shown that average entanglement over the unitarily invariant measure can be efficiently generated using random two-qubit operators in polynomial time. Hence, from the entanglement point of view as well, 'random circuits' is an important area of study. [3] However, haar random unitary operators are hard to implement from the circuit point of view. In order to implement a random haar unitary, we need an exponential number of two-qubit gates and random bits. Hence, it is useful to look at alternatives that can replace random unitaries. One such pseudo-random alternative is local random circuits. It has been shown that local random circuits composed of polynomial number of two-qubit gates form an approximate unitary t-design, i.e can approximately duplicate the properties of a non-local Haar uniform unitary [4].

It is known that random local gates are easier to implement than random non-local operators. Hence, alternatives to random quantum circuits have been discussed [7] where a fixed non-local operator is interlaced with random local unitaries. It was shown that such an interlacing of local gates leads to exponential growth of entanglement in time. Therefore, it is necessary to understand the entanglement properties of both fixed non-local unitaries and haar random local gates. Some of the work done so far on entanglement properties of random unitaries include 'effect of local dynamics' [7], 'comparing the entanglement properties of random diagonal unitaries with that of Haar random unitaries' [17], etc.

1.3   Outline of thesis

- In Chapter 2, we will introduce and quantify *operator entanglement*. The two main quantities under investigation *entangling power* (e_p) and *gate typicality* (g_t) are also explained. Also, we look at the effect of interlacing a fixed non-local unitary with haar random local gates.

- In Chapter 3, we shall look at the effect of local dynamics in a system of four qubits.

- In Chapter 4, we will look at the $e_p - g_t$ phase space diagrams of the four dimensional case and try to understand the boundaries of this space.

Chapter 2

Operator entanglement and effect of local dynamics

2.1 Overview

In this chapter we will mainly review the work done in [7] and [16]. In the last section of this chapter, we will reproduce some of these results and we will also see how it can be extended to a higher dimensional case.

The main focus of my project was to see if overall non-locality gets enhanced when non-local gate is iterated with random local gates in between and it is seen that on average, non-locality improves. In this work, we use linear entropy as a measure of non-locality. We use the operator Schmidt form of a unitary to define operator entanglement in terms of a reshuffled matrix. Then we define two complementary quantities : the *entangling power* (e_p) and *gate typicality* (g_t), and try to understand the dynamics using the $e_p - g_t$ phase space.

2.2 Theory

Here we use operator entanglement E(U) (defined in terms of linear entropy) as a measure of operator interaction strength. Consider a unitary gate U of order N^2 acting on composite Hilbert

space $\mathscr{H} = \mathscr{H}^N \otimes \mathscr{H}^N$. It's operator Schmidt form is [5]

$$U = \sum_{i=1}^{N^2} \sqrt{\lambda_i} A_i \otimes B_i \tag{2.1}$$

and the operator entanglement E(U) can be defined in terms of the Schmidt coefficients

$$E(U) = 1 - \frac{1}{N^4} \sum_{i=1}^{N^2} \lambda_i^2 \tag{2.2}$$

It is known that Schmidt coefficients of an operator U are the singular values of the reshuffled matrix U_R, i.e the positive square roots of eigenvalues of the operator $U_R U_R^\dagger$ or $U_R^\dagger U_R$. [6] Here, the reshuffled matrix U_R is defined to be $< ij \mid U_R \mid \alpha\beta > = < i\alpha \mid U \mid j\beta >$ If X is a 4*4 matrix then reshuffled form of X will be

$$X_R = \left[\begin{array}{cc|cc} X_{11} & X_{12} & X_{21} & X_{22} \\ X_{13} & X_{14} & X_{23} & X_{24} \\ \hline X_{31} & X_{32} & X_{41} & X_{42} \\ X_{33} & X_{34} & X_{43} & X_{44} \end{array} \right]$$

Hence, the rescaled squared Schmidt coefficients $\lambda_i' = \frac{\lambda_i}{N^2}$ are the eigenvalues of the density operator

$$\rho_R(U) = \frac{1}{N^2} U_R U_R^\dagger \tag{2.3}$$

The operator entanglement can thus be written as [7]

$$E(U) = 1 - tr(\,\rho_R^2(U)\,) \tag{2.4}$$

Similarly, we define another density operator ρ_T as

$$\rho_T(U) = \frac{1}{N^2}\, SU_T U_T^\dagger S \tag{2.5}$$

where U_T is the partial transposed matrix given by $< j\alpha \mid U_T \mid i\beta > = < i\alpha \mid U \mid j\beta >$ and S is the Swap operator of order N^2. As $S(SU)_R = U_T$, it is easy to relate eigenvalues of $\rho_T(U)$ to Schmidt

coefficients of (SU). It follows that

$$E(SU) = 1 - tr(\rho_T^2(U))$$

(2.6)

To understand the dynamics better using the phase space diagrams, it is useful to define the complementary quantities *entangling power* (e_p) and *gate typicality* (g_t). [7]

$$e_p(U) = \frac{N^2}{(N+1)^2}[E(U) + E(US) - E(S)]$$

(2.7)

$$g_t(U) = \frac{N^2}{N^2 - 1}[E(U) - E(US) + E(S)]$$

(2.8)

where $E(S) = \frac{N^2 - 1}{N^2}$. The entangling power e_p of a unitary of size N^2 is bounded as $0 \leq e_p \leq \frac{N-1}{N+1}$ and the g_t value ranges from 0 to 2. It is interesting to note that while e_p does not distinguish between Swap and local gates, g_t reaches its maximum value for Swap. Although $e_p(S) = 0$, the fact that $g_t(S) = 2$ indicates that Swap is a maximally non-local operator.

To distinguish between E(U) calculated using ρ_R and E(US) calculated using ρ_T, we can write the equations for e_p and g_t as

$$e_p(U) = \frac{N^2}{(N+1)^2}[E_R(U) + E_T(US) - E(S)]$$

(2.9)

$$g_t(U) = \frac{N^2}{N^2 - 1}[E_R(U) - E_T(US) + E(S)]$$

(2.10)

We should note here that when the partial transpose is taken across the first or second half of the system, the E(US) calculated using ρ_T and E(US) calculated using ρ_R give the same value.

Brief literature survey on entangling power

The entangling power of an operator was first defined in [8]. In this work, e_p is defined as

$$e_p(U) = \overline{E(U|\psi_1 > \otimes|\psi_2 >)}$$

(2.11)

where the bar denotes average over all product states and E is the entanglement measure (usually

linear entropy). Here, it is also proved that

$$e_p(U) = 2\,tr[U^{\otimes 2}\,\Omega_P\,U^{\dagger\,\otimes 2}\,P_{13}^-] \qquad (2.12)$$

where $\Omega_P = \int d\mu(\psi_1,\psi_2)(|\psi_1><\psi_1|\otimes|\psi_2><\psi_2|)^{\otimes 2}$ and P_{13}^- is the projector over the totally anti-symmetric subspace. Many properties of e_p are also discussed here like

1. $e_p(U_a \otimes U_b\,U) = e_p(U)$

2. $e_p(\mathbb{1}) = 0$ etc

It is important to note that e_p, g_t, E(U) and E(US) are all local-unitary invariants (LU invariant), i.e they do not change upon acting by just one set of local unitaries. They are truly capturing nonlocal properties of the operator. [7] [8]

In [11], study of e_p of permutation matrices has been done. They describe explicitly, methods to construct permutation matrices which have maximum and minimum e_p values. In [18], they show how to compute the entangling power of U using parametrization of U. They also formulate the entangling power of bipartite unitary operations of Schmidt rank two for any dimensions.

2.3   Interlacing local gates

A unitary gate U acting on composite Hilbert space $\mathscr{H}_N^A \otimes \mathscr{H}_N^B$ is said to be local if it can be written in the product form $U = U^A \otimes U^B$ where U^A and U^B act on $\mathscr{H}^A$ and $\mathscr{H}^B$ respectively. As we know, local gates do not create any entanglement and hence non-local gates are required. But since implementing non-local gates is difficult from the circuit point of view, it is useful to find an alternative using local gates. It was recently shown in [7] that when repeated actions of a fixed non-local unitary is interlaced with haar random local unitaries, non-locality on an average improves compared to the case with only non-local gates.

Consider an operator of the form

$$V = U\,(U_A^1 \otimes U_B^1)\,U\,(U_A^2 \otimes U_B^2)\,U........U\,(U_A^n \otimes U_B^n)\,U \qquad (2.13)$$

where U is a fixed unitary of order N^2 and $U_A^{i\,\prime}s$ and $U_B^{i\,\prime}s$ are unitaries of order N chosen according to Haar measure. In general, non-locality of V can be more or less than U depending on the local

gates, but on an average, non-locality improves when we interlace the non-local operator with random local unitaries.

For N=2 (two qubits) case, we consider the operator $V = \sqrt{U}(U_A \otimes U_B)\sqrt{U}$ and plot the E(VS) vs E(V) and g_t vs e_p phase space plots (fig 2.1). Each point in the phase space corresponds to one pair of U_A and U_B chosen according to haar measure. When the U is a fixed 4×4 haar random unitary, it can be clearly seen that in general, there exist local unitaries U_A and U_B such that the entangling power and gate typicality of V is more than that of U.

(a) E(VS) vs E(V)

(b) $g_t(V)$ vs $e_p(V)$

Figure 2.1: Phase space plots for 2 qubits. Values at each point are calculated for $V = \sqrt{U}(U_a \otimes U_b)\sqrt{U}$ where U is a fixed Haar random unitary operator. Each point corresponds to a different set of U_a and U_b. The red dot corresponds to U.

In the case of U = CNOT (where $CNOT = |0><0| \otimes \mathbb{1} + |1><1| \otimes \sigma_x$), it is seen that there does not exist any local unitaries U_A and U_B such that the entangling power and gate typicality of V is more than that of U (fig 2.2). This is consistent with the fact that CNOT is capable of maximally entangling qubits.

It was also observed that the entangling power averaged over an ensemble of local interlacing gates, gets enhanced with the number of iterations of U interlaced with the local gates and converges exponentially to the average e_p value given by $\bar{e}_p = \dfrac{(N-1)^2}{N^2+1}$ (fig 2.3). It is seen that similar behaviour is obtained even when the same local gates are applied at every iteration i.e $V = (\,(U_A \otimes U_B)\,U\,)^n$. The gate typicality g_t also exhibits similar trend and converges exponen-

(a) E(VS) vs E(V)

(b) $g_t(V)$ vs $e_p(V)$

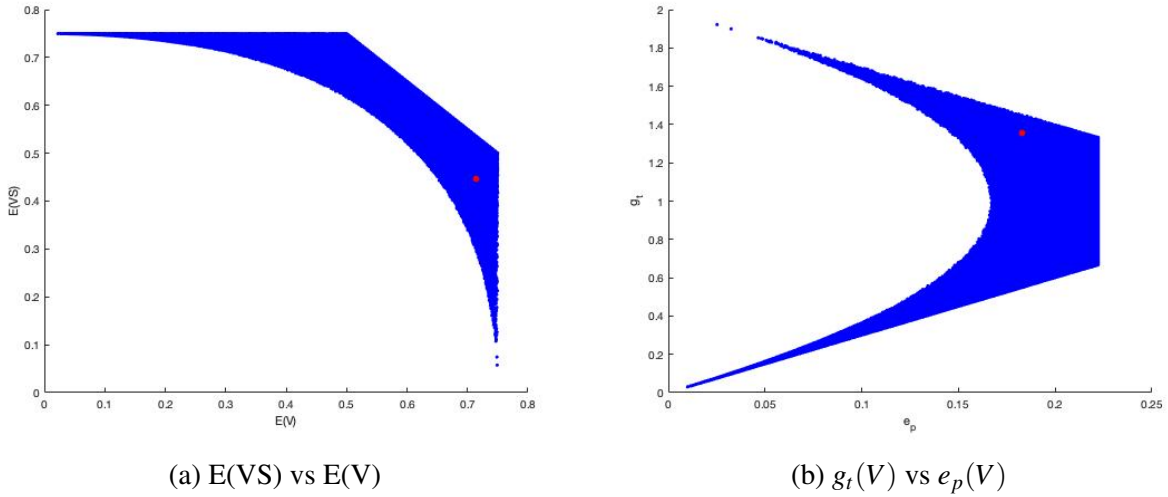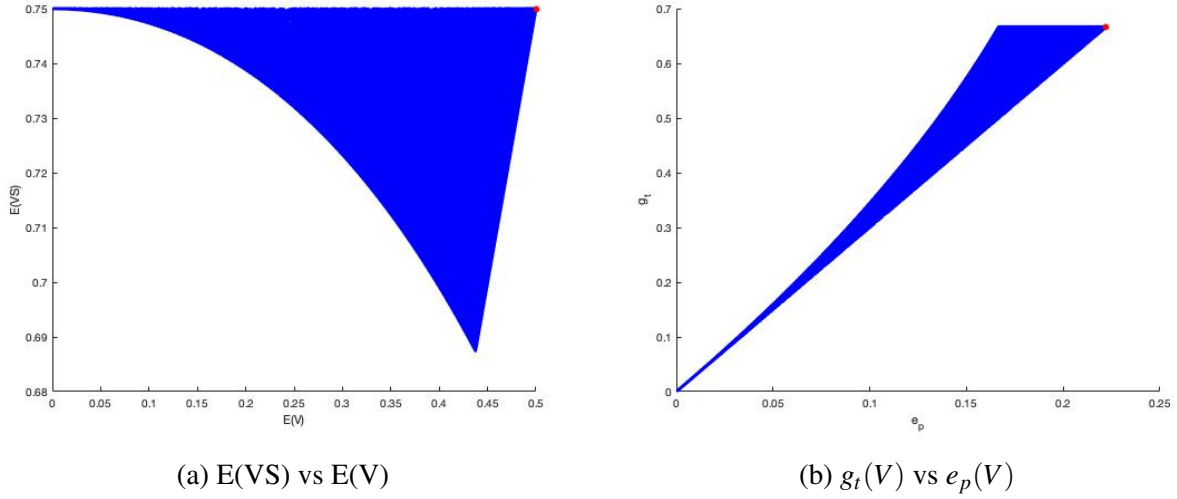Figure 2.2: Phase space plots for 2 qubits. Values at each point are calculated for $V = \sqrt{U}(U_a \otimes U_b)\sqrt{U}$ where U is CNOT. Each point corresponds to a different set of U_a and U_b. The red dot corresponds to U.

tially to its asymptotic value.
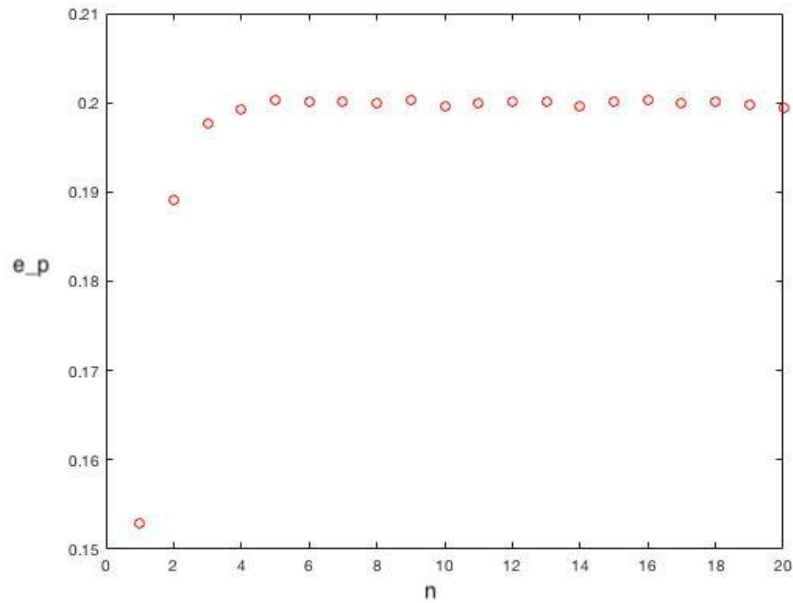
Figure 2.3: Entangling power e_p after n iterations of U interlaced with random local gates ; plotted for N=2. Values are averaged over local gates

Consider N=2 qubit system. It has been shown that the phase space of haar random unitaries $U(N^2)$ is same as that of $V = \sqrt{U}(U_a \otimes U_b)\sqrt{U}$. It is clear that local gates interlaced between a fixed non-local U have the ability of creating as much entanglement as that of random non-local operators, with the right choice of local unitaries. This result provides great advantage as it helps in achieving the same extent of entanglement but with lesser circuit complexity.

2.4 4 qubit system

Problem of interest

In [2] and [15], random quantum circuits (RUC's) have been discussed in detail. Here, RUCs are defined as *"minimally structured models of quantum chaotic dynamics; they generate random time evolution, subject only to spatial locality"*. These random quantum circuits have alternating random, bipartite (nonlocal) unitaries in each time step. But as we know nonlocal random gates are hard to implement. Hence, we study what happens when there are fixed nonlocal unitaries but random locals at intermediate steps. Here, we will extend the work done in [7] to a 4 qubit system.

For the 4 qubit case, our system of interest is as follows :

A1   A2   B1   B2

We are interested in calculating the operator entanglement across the $A_1A_2 \mid B_1B_2$ cut. For example, we will consider the operator $V = \sqrt{U}(U_a \otimes U_b)\sqrt{U}$ where U is the non-local operator in the first time step, U_a and U_b are the local random gates in the second time step and then in the third time step, again we have the non-local operator.

time step 3

time step 2

time step 1
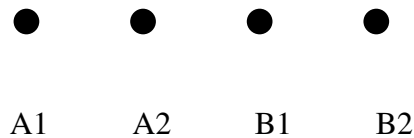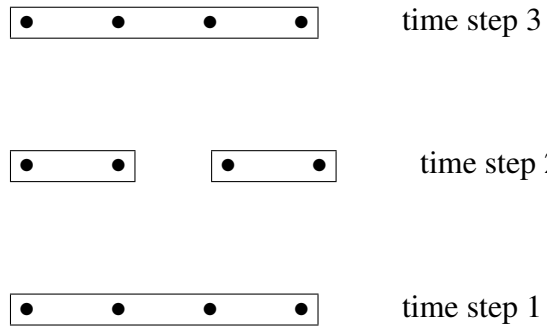
Here the dots represent the qubits and the boxes represent the operators acting on it. Note that the above figure represents just one way of interlacing locals between nonlocals. We can also try different combinations like having 4 single qubit gates in 2nd time step, or having the non-locals itself in a product form (as long as non-locality across $A_1 A_2 \mid B_1 B_2$ cut is preserved), etc.

12

Chapter 3

Boundaries of the $e_p - g_t$ phase space

It is interesting to look at the $e_p - g_t$ phase space and identify the curves that form the boundaries. It is also useful to try and identify the family of gates corresponding to these boundary curves, as it will give an idea of the entanglement properties of different set of operators.

As mentioned before he phase space of haar random unitaries $U(N^2)$ is same as that of $V = \sqrt{U}(U_a \otimes U_b)\sqrt{U}$, where the local gates are Haar random unitaries. Hence, in this chapter we will be looking at the $e_p - g_t$ phase space of $U(N^2)$ chosen according to Haar measure and identifying the boundaries of the same.

3.1 2 qubit system

It has been shown in [14] that the left, right, top and bottom boundaries of the 2 qubit phase space are the $e_p - g_t$ curves for S^{α}, $(CNOT)S^{\alpha}$, $S(CNOT)^{\alpha}$ and $CNOT^{\alpha}$ respectively, where $0 \leq \alpha \leq 1$. The bounds for e_p and g_t were analytically derived and it was found to match the curves for the aforementioned gates. (fig 3.1)

It should be noted that the maximum value of g_t is 2 which is attained only by Swap and its local equivalents. The minimum value 0 is attained by just the local operators. The maximum value attainable by e_p is $\frac{1}{3}$ but here, it does not exceed $\frac{2}{9}$ which is the e_p value for CNOT gate. It

is consistent with the fact that for the 2 qubit case, the optimal value for e_p is $\frac{2}{9}$ and thus CNOT is an optimal operator for the $N = 2$. [8] It is also interesting to note that a natural $N > 2$ dimensional generalization of the CNOT gate is not optimal, which we will demonstrate in the next section for the 4 qubit case.
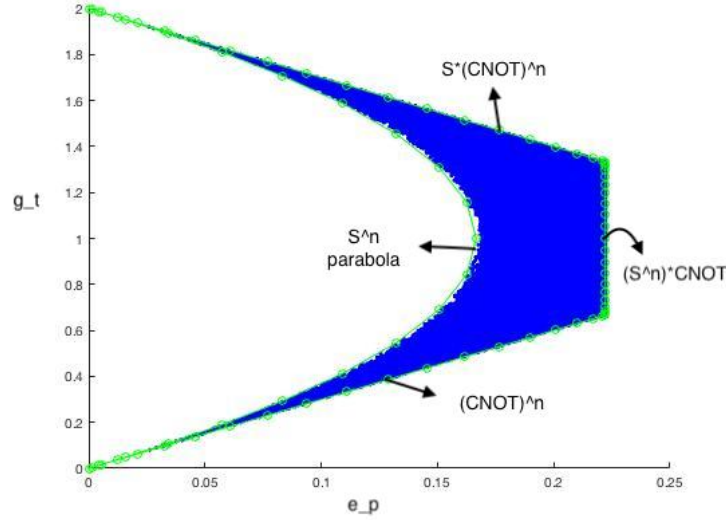
Figure 3.1: g_t vs e_p phase space for $N = 2$, with the boundaries marked with the corresponding gates

3.2   4 qubit system

Boundaries

We extend the set of gates that form the boundaries of the 2 qubit phase space to the 4 qubit case and try to verify if they indeed give us the boundaries of the 4 qubit phase space. S is the 4 qubit Swap operator defined as

$$S = \sum_{i,j,k,l=0}^{1} |ijkl><klij| \tag{3.1}$$

The 4 dimensional generalization of CNOT id defined as [9]

$$CNOT\,|\,x>|\,y>=|\,x>|-x-y> \tag{3.2}$$

14

where $|x>, |y> \in \{|0>, ..., |N-1>\}$ and $|-x-y>$ is the state $|(-x-y) \bmod N>$ and here N=4. Note that though this definition of CNOT is for two 4-dimensional qudits, we can obtain the same operator by extending it the 4 qubits case. Using these operators, when we plot the $e_p - g_t$ curves similar to the 2 qubit case, we get fig 3.2. But we need to analytically verify if this is actually the boundary of the phase space.
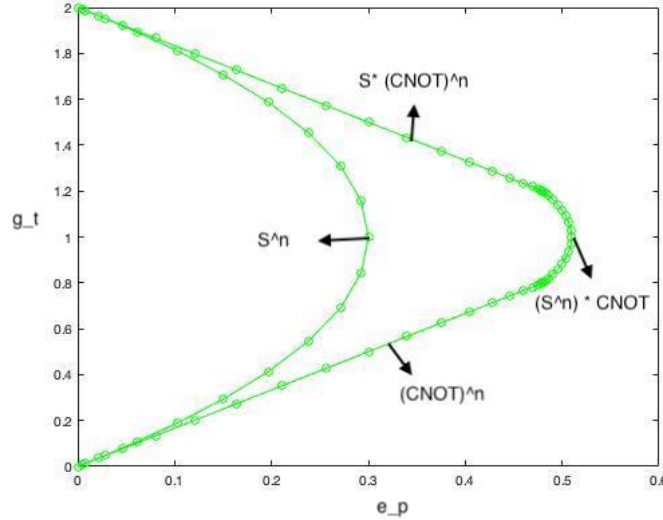
Figure 3.2: Expected boundaries for N=4 g_t vs e_p phase space

Top and bottom bounds

To derive the top and bottom bounds of the phase space, we shall write E(U) and E(US) in terms of e_p and g_t and then use the maximum value of E(U) to obtain bounds on g_t. Then we verify whether these match with the $e_p - g_t$ curves of $S(CNOT)^\alpha$ (for the upper bound on g_t) and $CNOT^\alpha$ (for the lower bound on g_t) as we expect it to be.

For N=4, $E(S) = \dfrac{N^2 - 1}{N^2} = \dfrac{15}{16}$ and so e_p and g_t can be written as

$$e_p(U) = \frac{16}{25}[E(U) + E(US)] - \frac{3}{5} \tag{3.3}$$

$$g_t(U) = \frac{16}{25}[E(U) - E(US)] + 1 \tag{3.4}$$

15

Using this, E(U) and E(US) can be written in terms of e_p and g_t as:

$$E(U) = \frac{15}{32}[g_t(U) + \frac{5}{3}e_p(U)]$$ (3.5)

$$E(US) = \frac{5}{32}[5e_p(U) - 3g_t(U) + 6]$$ (3.6)

We know the upper bound of E(U) and E(US) is $\frac{N^2 - 1}{N^2}$ (equal to $\frac{15}{16}$) [7]. Using this and equations (3.5) and (3.6), we can calculate the following bounds :

$$g_t \leq 2 - \frac{5}{3}e_p$$ (3.7)

$$g_t \geq \frac{5}{3}e_p$$ (3.8)

These equations are found to be that of the top and bottom bounds of the phase space which exactly coincide with $e_p - g_t$ curves for $S(CNOT)^\alpha$ and $CNOT^\alpha$ family (fig 3.3).

Figure 3.3: Boundaries of g_t vs e_p phase space. Green lines represent the boundary calculated using powers of gates and red dots represent the lines given by eqns (3.7) and (3.8)
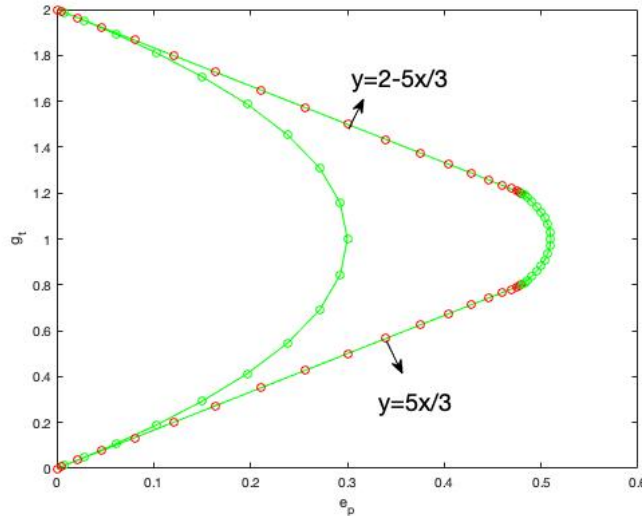
16

Entangling power of S^α family

To understand the left bound, we will analytically find out the equation of the parabola corresponding to the S^α family and verify whether it is a valid numeric bound on e_p. Here we use a method (described in [14]) where we define the Swap operator in terms of a pair of projectors and then analytically calculating $E(S^\alpha)$ and hence $e_p(S^\alpha)$ and $g_t(S^\alpha)$ in terms of $\omega_\alpha = \sqrt{-1}$. This will give a relation between e_p and g_t, which we expect to be the equation of the parabola.

The Swap gate $S(N^2)$ can be written as

$$S_{AB} = \prod^+_{AB} + \prod^-_{AB} \tag{3.9}$$

where $\prod^+_{AB}$ and $\prod^-_{AB}$ are symmetric and anti-symmetric projectors given by

$$\prod^+_{AB} = \frac{\mathbb{1}_{AB} + S_{AB}}{2} = \frac{1}{2} \sum_{k,\beta=0}^{N-1} [|k\beta\rangle\langle k\beta| + |k\beta\rangle\langle\beta k|] \text{ and}$$

$$\prod^-_{AB} = \frac{\mathbb{1}_{AB} - S_{AB}}{2} = \frac{1}{2} \sum_{k,\beta=0}^{N-1} [|k\beta\rangle\langle k\beta| - |k\beta\rangle\langle\beta k|]$$

Any power of S can be written as

$$S^\alpha = \prod^+_{AB} + (-1)^\alpha \prod^-_{AB} \equiv \prod^+_{AB} + \omega_\alpha \prod^-_{AB}$$

$$= \frac{1+\omega_\alpha}{2} \mathbb{1} + \frac{1-\omega_\alpha}{2} S$$

$$= \frac{1+\omega_\alpha}{2} \sum_{k,\beta=0}^{N-1} [|k\beta\rangle\langle k\beta| + \frac{1-\omega_\alpha}{2} \sum_{k,\beta=0}^{N-1} [|k\beta\rangle\langle\beta k|$$

A matrix element will have the form :

$$\langle i\gamma | S^\alpha | j\delta \rangle = \frac{1+\omega_\alpha}{2} \delta_{ij}\delta_{\gamma\delta} + \frac{1-\omega_\alpha}{2} \delta_{i\delta}\delta_{j\gamma}$$

Similarly, the elements of realigned and partial transposed matrix are

$$\langle i\gamma | S^\alpha_R | j\delta \rangle = \langle ij | S^\alpha | \gamma\delta \rangle = \frac{1+\omega_\alpha}{2} \delta_{i\gamma}\delta_{j\delta} + \frac{1-\omega_\alpha}{2} \delta_{i\delta}\delta_{j\gamma}$$

17

$$< i\gamma \,|\, S_T^\alpha \,|\, j\delta > = < j\gamma \,|\, S^\alpha \,|\, i\delta > = \frac{1+\omega_\alpha}{2}\delta_{ij}\delta_{\gamma\delta} + \frac{1-\omega_\alpha}{2}\delta_{i\gamma}\delta_{j\delta}$$

Operator entanglement of S^α is given by

$$E(S^\alpha) \quad = \quad 1 - \frac{1}{N^4}tr(S_R^\alpha S_R^{\alpha^\dagger} S_R^\alpha S_R^{\alpha^\dagger}) \tag{3.10}$$

$$\tag{3.11}$$

$$= \quad 1 - \frac{1}{N^4} < i\beta \,|\, S_R^\alpha \,|\, m_1\gamma_1 >< m_2\gamma_2 \,|\, S_R^\alpha \,|\, m_1\gamma_1 >^* < m_2\gamma_2 \,|\, S_R^\alpha \,|\, m_3\gamma_3 >< i\beta \,|\, S_R^\alpha \,|\, m_3\gamma_3 >^* \tag{3.12}$$

$$= 1 - \frac{1}{16N^4}[(1+\omega_\alpha)\delta_{i\beta}\delta_{m_1\gamma_1} + (1-\omega_\alpha)\delta_{\beta m_1}\delta_{i\gamma_1}][(1+\omega_\alpha^*)\delta_{m_1\gamma_1}\delta_{m_2\gamma_2} + (1-\omega_\alpha^*)\delta_{m_1\gamma_2}\delta_{m_2\gamma_1}][(1+$$
$$\omega_\alpha)\delta_{m_2\gamma_2}\delta_{m_3\gamma_3} + (1-\omega_\alpha)\delta_{m_2\gamma_3}\delta_{\gamma_2 m_3}][(1+\omega_\alpha^*)\delta_{i\beta}\delta_{m_3\gamma_3} + (1-\omega_\alpha^*)\delta_{i\gamma_3}\delta_{\beta m_3}]$$

After performing $\sum_{m_1,\gamma_1}$ and $\sum_{m_3,\gamma_3}$,

$$E(S^\alpha) = 1 - \frac{1}{16N^4}[N(1+\omega_\alpha)(1+\omega_\alpha^*)\delta_{i\beta}\delta_{m_2\gamma_2} + (1+\omega_\alpha)(1-\omega_\alpha^*)\delta_{i\beta}\delta_{m_2\gamma_2}]^2[(1-$$
$$\omega_\alpha)(1+\omega_\alpha^*)\delta_{i\beta}\delta_{m_2\gamma_2} + (1-\omega_\alpha)(1-\omega_\alpha^*)\delta_{\beta\gamma_2}\delta_{im_2}]^2$$

Summing over rest of the indices,

$$E(S^\alpha) = 1 - \frac{1}{16N^2}[N^2(1+\omega_\alpha)^2(1+\omega_\alpha^*)^2 + (1+\omega_\alpha)^2(1-\omega_\alpha^*)^2 + (1-\omega_\alpha)^2(1+$$
$$\omega_\alpha^*)^2 + (1-\omega_\alpha)^2(1-\omega_\alpha^*)^2 + 4(1-\omega_\alpha^2)(1-\omega_\alpha^{*2})]$$

Writing $\omega_\alpha = (-1)^\alpha = e^{i\alpha\pi(2k+1)}$ and using the fact $|\omega_\alpha|^2 = 1$, we get

$$E(S^\alpha) \quad = \quad \frac{1}{4N^2}[3N^2 - 2 - 2(N^2-1)cos((2k+1)\alpha\pi) - N^2cos^2((2k+1)\alpha\pi) -$$
$$sin^2((2k+1)\alpha\pi)]$$

$$= \quad \frac{N^2-1}{2N^2}[\frac{1}{2}sin^2((2k+1)\alpha\pi) + 1 - cos((2k+1)\alpha\pi)]$$

$$= \quad \frac{N^2-1}{N^2}sin^2(\frac{(2k+1)\alpha\pi}{2})[1 + cos^2(\frac{(2k+1)\alpha\pi}{2})]$$

Operator entanglement of $S^\alpha S$ would be

18

$$E(S^\alpha S) = E(S^{\alpha+1}) = \frac{N^2-1}{N^2}\cos^2(\frac{(2k+1)\alpha\pi}{2})[1+\sin^2(\frac{(2k+1)\alpha\pi}{2})]$$

Now for the N = 4 case, entangling power and gate-typicality is given by

$$e_p(S_k^\alpha) = \frac{N^2}{(N+1)^2}[E(S_k^\alpha) + E(S_k^\alpha S) - E(S)]$$

$$= \frac{N^2}{(N+1)^2}[\frac{N^2-1}{N^2}\sin^2(\frac{(2k+1)\alpha\pi}{2})(1+\cos^2(\frac{(2k+1)\alpha\pi}{2})) + \frac{N^2-1}{N^2}\cos^2(\frac{(2k+1)\alpha\pi}{2})(1+$$

$$\sin^2(\frac{(2k+1)\alpha\pi}{2})) - \frac{N^2-1}{N^2}]$$

$$= \frac{N-1}{2(N+1)}\sin^2((2k+1)\alpha\pi)$$

$$= \frac{3}{10}\sin^2((2k+1)\alpha\pi)$$

$$g_t(S_k^\alpha) = \frac{N^2}{N^2-1}[E(S_k^\alpha) - E(S_k^\alpha S) + E(S)]$$

$$= \frac{N^2}{N^2-1}[\frac{N^2-1}{N^2}\sin^2(\frac{(2k+1)\alpha\pi}{2})(1+\cos^2(\frac{(2k+1)\alpha\pi}{2})) - \frac{N^2-1}{N^2}\cos^2(\frac{(2k+1)\alpha\pi}{2})(1+$$

$$\sin^2(\frac{(2k+1)\alpha\pi}{2})) + \frac{N^2-1}{N^2}]$$

$$= \sin^2(\frac{(2k+1)\alpha\pi}{2}) - \cos^2(\frac{(2k+1)\alpha\pi}{2}) + 1$$

$$= 2\sin^2(\frac{(2k+1)\alpha\pi}{2})$$

Now,

$$\frac{3}{10}g_t(2 - g_t) = \frac{3}{10}2\sin^2(\frac{(2k+1)\alpha\pi}{2})(2 - 2\sin^2(\frac{(2k+1)\alpha\pi}{2}))$$

$$= \frac{3}{10}\sin^2((2k+1)\alpha\pi) = e_p$$

Hence, $\boxed{\frac{3}{10}g_t(2-g_t) = e_p}$ is the equation that defines the parabola of the S^α family.

This suggests that the lower bound on e_p should be given by $e_p \geq \dfrac{3}{10} g_t(2 - g_t)$. In the simulations we observe that every gate satisfies this inequality.

As a future prospect, we can try to derive a lower bound on e_p using the Khaneja Glaser decomposition (see [10]) of U(16) and 'local invariants' and we expect it to be the above equation. Then we can conclude that $e_p - g_t$ curve corresponding to S^α family forms the left boundary of the 4 qubit $e_p - g_t$ phase space.

Entangling power of $(CNOT)S^\alpha$ family

Now we shall look at the equation of the $e_p - g_t$ curve of $(CNOT)S^\alpha$ family and verify if it can form the right boundary. A similar derivation has been done in [14].

Recall from the previous section that any power of S can be written as

$$S^\alpha = \frac{1 + \omega_\alpha}{2}\mathbb{1} + \frac{1 - \omega_\alpha}{2}S$$

For N=4, this can be expanded as

$$S^\alpha = |00><00| + |11><11| + |22><22| + |33><33| + \frac{1 + \omega_\alpha}{2}[|01><01| +$$
$|02><02| + |03><03| + |10><10| + |12><12| + |13><13| + |20><20| + |21><$
$21| + |23><23| + |30><30| + |31><31| + |32><32|] + \dfrac{1 - \omega_\alpha}{2}[|01><10| + |02><$
$20| + |03><30| + |10><01| + |12><21| + |13><31| + |20><02| + |21><$
$12| + |23><32| + |30><03| + |31><13| + |32><23|]$

A higher dimensional CNOT is given by [9] :

$$CNOT \,|\, x > |\, y >= |\, x > |-x - y >$$

where $|\, x >, |\, y > \in \{|\, 0 >, ..., |\, N - 1 >\}$ and $|-x - y >$ is the state $|(-x - y) \bmod N>$

Hence for the 4-dimensional case, CNOT will be

$$C \equiv CNOT = |00><00| + |01><03| + |02><02| + |03><01| + |10><$$
$$13| + |11><12| + |12><11| + |13><10| + |20><22| + |21><21| + |22><$$
$$20| + |23><23| + |30><31| + |31><30| + |32><33| + |33><32|$$

Now, the reshuffled matrix of CS^α would be

$$(CS^\alpha)_R = |00><00| + |11><21| + |22>02| + |33><23| + \frac{1+\omega_\alpha}{2}[|00><$$
$$13| + |00><22| + |00><31| + |11><03| + |11><12| + |11><30| + |22><$$
$$11| + |22><20| + |22><33| + |33><01| + |33><10| + |33><32|] + \frac{1-\omega_\alpha}{2}[|03><$$
$$10| + |02><20| + |01><30| + |13><01| + |12><11| + |10><31| + |21><$$
$$12| + |20><22| + |23><32| + |31><03| + |30><13| + |32><33|]$$

Writing $\omega_\alpha = (-1)^\alpha = e^{i\alpha\pi(2k+1)} = cos(\alpha\pi(2k+1)) + isin(\alpha\pi(2k+1))$, we get

$$tr[\,\{\,(CS^\alpha)_R(CS^\alpha)_R^\dagger\,\}^2\,] = 4\,(\,3cos^2(\frac{\alpha\pi(2k+1)}{2})+1)^2 - 24(\frac{i}{2}sin(\alpha\pi(2k+1))\,)^2 +$$
$$12sin^4(\frac{\alpha\pi(2k+1)}{2})$$

$$= 4\,(\,3cos^2(\frac{\alpha\pi(2k+1)}{2})+1)^2 + 12(1 - cos^2(\frac{\alpha\pi(2k+1)}{2})\,)^2 + 6(\,2\,sin(\frac{\alpha\pi(2k+1)}{2})\,cos(\frac{\alpha\pi(2k+}{2}$$

$$= 24\,cos^2(\frac{\alpha\pi(2k+1)}{2})\,(\,1+cos^2(\frac{\alpha\pi(2k+1)}{2})\,)\,) + 16$$

$$= 6\,(1+cos(\alpha\pi(2k+1)))\,(3+cos(\alpha\pi(2k+1))) + 16$$

Using this we can now calculate the operator entanglement $E(CS^\alpha)$

$$E(CS^\alpha) = 1 - tr[\rho_R^2(CS^\alpha)\,]$$

$$= 1 - \frac{1}{N^4}tr[\,\{\,(CS^\alpha)_R(CS^\alpha)_R^\dagger\,\}^2\,]$$

$$= 1 - \frac{1}{128}(\,3(3 + 4cos(\alpha\pi(2k+1)) + cos^2(\alpha\pi(2k+1))\,) + 8)$$

$$E(CS^\alpha\,S) = E(CS^{\alpha+1})$$

$$= 1 - \frac{1}{128}(\; 3(3 \; - \; 4cos(\alpha\pi(2k+1)) \; + \; cos^2(\alpha\pi(2k+1)) \;) \; +8)$$

Calculating the entangling power and gate typicality using these, we get

$$e_p(CS^\alpha) = \frac{N^2}{(N+1)^2}[E(CS^\alpha) + E(CS^{\alpha+1}) - E(S)]$$

$$= \frac{16}{25}[\; 2 \; - \; \frac{1}{128}\{3(6 \; + \; 2cos^2(\alpha\pi(2k+1)) \;) \; + \; 16\} \; - \; \frac{15}{16}]$$

$$= \frac{3}{5}[1 \; - \; \frac{1}{20}(3 \; + \; cos^2(\alpha\pi(2k+1)) \;)]$$

and

$$g_t(CS^\alpha) = \frac{N^2}{N^2-1}[E(CS^\alpha) - E(CS^{\alpha+1}) + E(S)]$$

$$= \frac{16}{15}[\frac{-1}{128} \; 24cos(\alpha\pi(2k+1)) \; + \; \frac{15}{16}]$$

$$= 1 - \frac{1}{5}cos(\alpha\pi(2k+1))$$

From the expression for g_t, we get

$$cos(\alpha\pi(2k+1)) = 5(1 - g_t)$$

Substituting this in equation for e_p,

$$e_p = \frac{3}{5}[1 \; - \; \frac{1}{20}(3 \; + \; 25(1 \; - \; g_t)^2 \;)]$$

$$= \frac{-3}{4}g_t \; (g_t - 2) \; - \; \frac{6}{25}$$

Hence $\boxed{e_p = \dfrac{-3}{4}g_t \; (g_t - 2) \; - \; \dfrac{6}{25}}$ is the equation that defines the parabola of CS^α family.

This suggests that the upper bound on e_p should be given by $e_p \leq \dfrac{-3}{4}g_t \; (g_t - 2) - \dfrac{6}{25}$. But

note that the average value of e_p is given by $\dfrac{(N-1)^2}{(N^2+1)}$ and for N=4, it takes the value 0.529. It is clearly easy to find a unitary , that has $e_p = 0.529$ and $g_t = 1$ (average g_t value). But according to the inequality, when $g_t = 1$, the maximum value e_p can take is 0.51 i.e $e_p \leq 0.51$. So clearly there exists at least one unitary that violates this inequality and hence we can conclude that the curve corresponding to CS^α does not form the right boundary of the 4 qubit phase space. This is consistent with the fact that for $N > 2$, the generalizations of CNOT gate are not optimal operators. [8]

3.3   Identifying gates with maximum and minimum e_p

In order to figure out the right boundary, it might be useful to identify the unitary with maximum e_p value. This will give us an idea about what kind of gates are optimal and what the maximum attainable value of e_p for each dimension is.

Maximum e_p

A method to construct permutation matrices/operators with maximum entangling power (in every dimension) has been shown. Using this we shall construct an optimal unitary (in this case, a permutation matrix) and check whether it can attain the maximum e_p value $\dfrac{3}{5}$ (for $N = 4$).

   A permutation matrix P of order N^2 is a square binary matrix that has exactly one entry of 1 in each row and each column and 0's elsewhere. When P is multiplied with another matrix A, it ends up permuting the rows or columns of A. It is also known that a latin square of side N is a $N \times N$ matrix with entries from the set $[N] = 1,.....,N$ such that every row and column is a permutation of $1,....,N$ and two $N \times N$ latin squares (k_{ij}) and (l_{ij}) orthogonal if $(k_{ij}$, $l_{ij})$ is a permutation of $[N] \times [N]$.

Now let P be a permutation matrix defined by [11]

$$P(|i> |j>) \; = \; |k_{ij}> |l_{ij}> \tag{3.13}$$

Then the entangling power of P equals the maximum value $\dfrac{N-1}{N+1}$ if and only if the matrices (k_{ij}) and (l_{ij}) are orthogonal latin squares. It follows that a permutation matrix P has maximum entan-

gling power if and only if $\tilde{P}$ is obtained by superimposing two orthogonal latin squares. Here $\tilde{P}$ is an $N \times N$ array used to represent the $N^2 \times N^2$ matrix P where $(ij)^{th}$ cell of $\tilde{P}$ is of the form (k_{ij}, l_{ij}) and $K = k_{ij}$ & $L = l_{ij}$ are orthogonal latin squares.

For the 4 dimensional case, one pair orthogonal latin squares is given by

$$K = \begin{bmatrix} 1 & 2 & 3 & 4 \\ 2 & 1 & 4 & 3 \\ 3 & 4 & 1 & 2 \\ 4 & 3 & 2 & 1 \end{bmatrix} \quad \text{and} \quad L = \begin{bmatrix} 1 & 2 & 3 & 4 \\ 3 & 4 & 1 & 2 \\ 4 & 3 & 2 & 1 \\ 2 & 1 & 4 & 3 \end{bmatrix}$$

Hence, $\tilde{P} = \begin{bmatrix} 11 & 22 & 33 & 44 \\ 23 & 14 & 41 & 32 \\ 34 & 43 & 12 & 21 \\ 42 & 31 & 24 & 13 \end{bmatrix}$ i.e

$$P = \left[\begin{array}{cccc|cccc|cccc|cccc} 1 & 0 & 0 & 0 & 0 & 0 & 0 & 0 & 0 & 0 & 0 & 0 & 0 & 0 & 0 & 0 \\ 0 & 0 & 0 & 0 & 0 & 1 & 0 & 0 & 0 & 0 & 0 & 0 & 0 & 0 & 0 & 0 \\ 0 & 0 & 0 & 0 & 0 & 0 & 0 & 0 & 0 & 0 & 1 & 0 & 0 & 0 & 0 & 0 \\ 0 & 0 & 0 & 0 & 0 & 0 & 0 & 0 & 0 & 0 & 0 & 0 & 0 & 0 & 0 & 1 \\ \hline 0 & 0 & 0 & 0 & 0 & 0 & 0 & 1 & 0 & 0 & 0 & 0 & 0 & 0 & 0 & 0 \\ 0 & 0 & 1 & 0 & 0 & 0 & 0 & 0 & 0 & 0 & 0 & 0 & 0 & 0 & 0 & 0 \\ 0 & 0 & 0 & 0 & 0 & 0 & 0 & 0 & 0 & 0 & 0 & 0 & 0 & 1 & 0 & 0 \\ 0 & 0 & 0 & 0 & 0 & 0 & 0 & 0 & 1 & 0 & 0 & 0 & 0 & 0 & 0 & 0 \\ \hline 0 & 0 & 0 & 0 & 0 & 0 & 0 & 0 & 0 & 1 & 0 & 0 & 0 & 0 & 0 & 0 \\ 0 & 0 & 0 & 0 & 0 & 0 & 0 & 0 & 0 & 0 & 0 & 0 & 1 & 0 & 0 & 0 \\ 0 & 0 & 0 & 1 & 0 & 0 & 0 & 0 & 0 & 0 & 0 & 0 & 0 & 0 & 0 & 0 \\ 0 & 0 & 0 & 0 & 0 & 0 & 1 & 0 & 0 & 0 & 0 & 0 & 0 & 0 & 0 & 0 \\ \hline 0 & 0 & 0 & 0 & 0 & 0 & 0 & 0 & 0 & 0 & 0 & 0 & 0 & 0 & 1 & 0 \\ 0 & 0 & 0 & 0 & 0 & 0 & 0 & 0 & 0 & 0 & 0 & 1 & 0 & 0 & 0 & 0 \\ 0 & 0 & 0 & 0 & 1 & 0 & 0 & 0 & 0 & 0 & 0 & 0 & 0 & 0 & 0 & 0 \\ 0 & 1 & 0 & 0 & 0 & 0 & 0 & 0 & 0 & 0 & 0 & 0 & 0 & 0 & 0 & 0 \end{array} \right] \qquad (3.14)$$

This permutation matrix has $e_p = \dfrac{3}{5}$ which is the maximum possible value for entangling power for N=4.

Minimum e_p

To identify a permutation matrix P with the least non-zero entangling power, a new array representation $\hat{P}$ was introduced. If $(ij)^{th}$ cell of $\hat{P}$ is kl, then in P, the contribution of $|kl >< ij|$ term is non-zero. It was shown that for a permutation matrix P, e_p is non-zero but minimum over all permutations if [11]

$$\hat{P} = \begin{bmatrix} 11 & 12 & .. & .. & 1N \\ 21 & 22 & .. & .. & 2N \\ .. & .. & .. & .. & .. \\ N1 & N2 & .. & NN & N(N-1) \end{bmatrix} \tag{3.15}$$

For N=4, it will be

$$\hat{P} = \begin{bmatrix} 11 & 12 & 13 & 14 \\ 21 & 22 & 23 & 24 \\ 31 & 32 & 33 & 34 \\ 41 & 42 & 44 & 43 \end{bmatrix} \tag{3.16}$$

The permutation matrix corresponding to this $\hat{P}$ has $e_p = 0.18$ which is the minimum but non-zero value for entangling power for N=4.

Chapter 4

Simulations using different sets of gates

In this chapter we will look at $E(VS)$ vs $E(V)$ and g_t vs e_p phase space diagrams for different sets and combinations of non-local and local gates, for $N = 4$. In the phase space plots, we consider operators of the form

$$V = (\text{ fixed non-local operator }) * (\text{random local gates}) * (\text{ fixed non-local operator })$$

Each phase space plot helps in understanding the entanglement properties of the corresponding combination of operators. By comparing the plots, we can obtain a clear idea about the effect of different combinations of haar random local operators on the entangling power and gate typicality.

As mentioned in the previous chapter, we are interested in the entanglement across the A-B cut i.e across the first and second halves of the 4 qubit system. Hence, the non-local operators can be in a product form as well, as long as there is some non-local part acting across the A-B cut. For example, in this work,we will look at 2 cases of the non-local operator:

- $A_{2 \times 2} \otimes B_{4 \times 4} \otimes C_{2 \times 2}$

- $A_{16 \times 16}$

And for the haar random local gates, we consider the following combinations :

- $U_{2 \times 2}^{A1} \otimes U_{2 \times 2}^{A2} \otimes U_{2 \times 2}^{B1} \otimes U_{2 \times 2}^{B2}$
- $U_{4 \times 4}^{A} \otimes U_{4 \times 4}^{B}$

4.1 When the non-local operator is in product form

4.1.1 Case 1

$$V = (\mathbb{1} \otimes U \otimes \mathbb{1}) * (Ua \otimes Ub) * (\mathbb{1} \otimes U \otimes \mathbb{1})$$

where U is a fixed 4*4 unitary, $\mathbb{1}$ is the 2*2 identity, Ua and Ub are 4*4 bipartite unitaries.
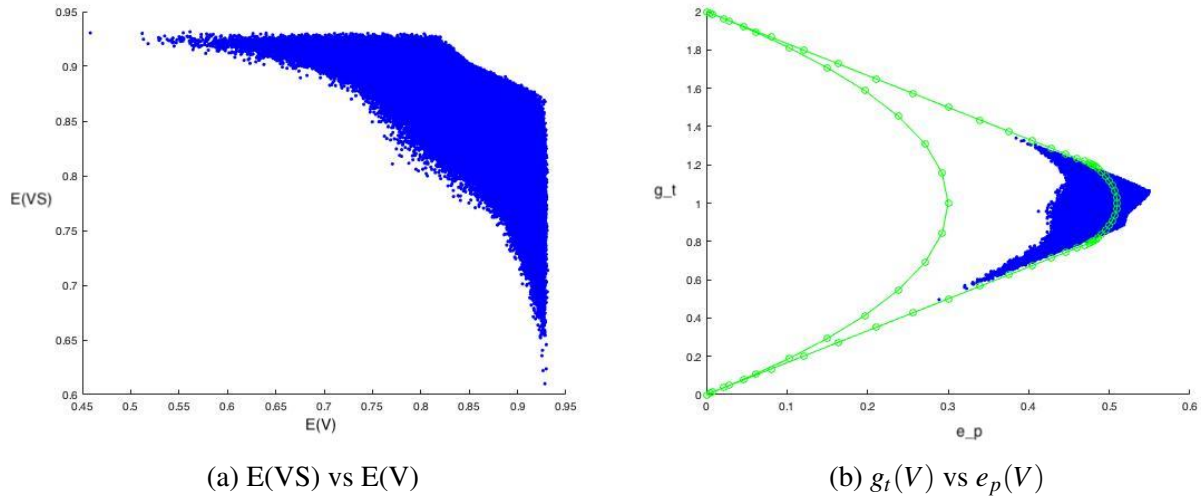
When U is a Haar random unitary :

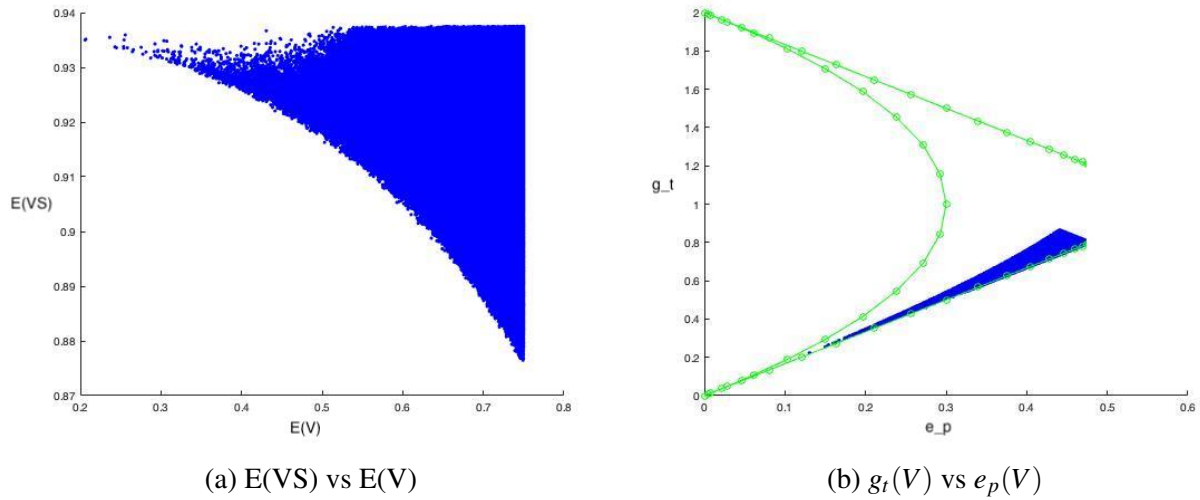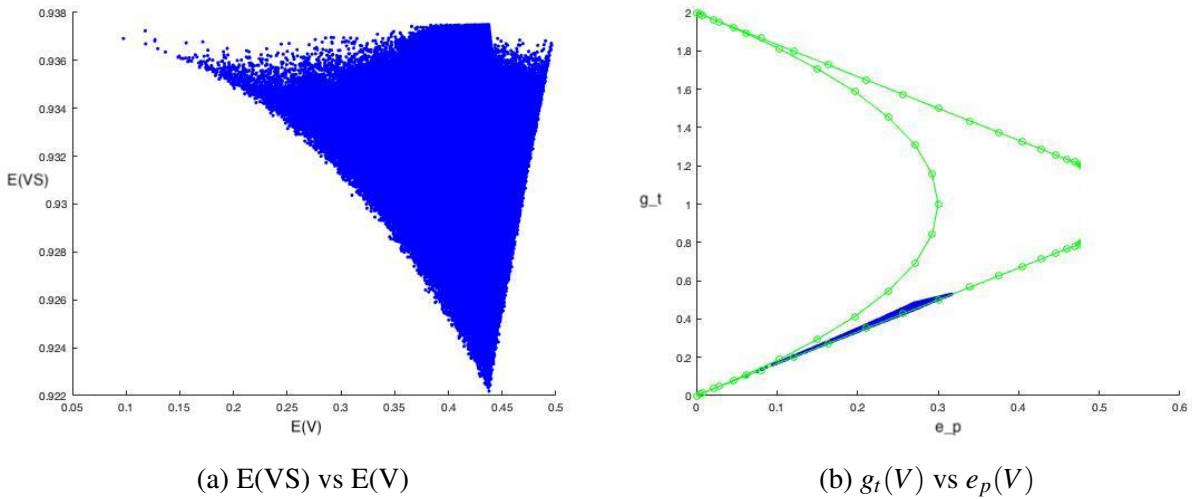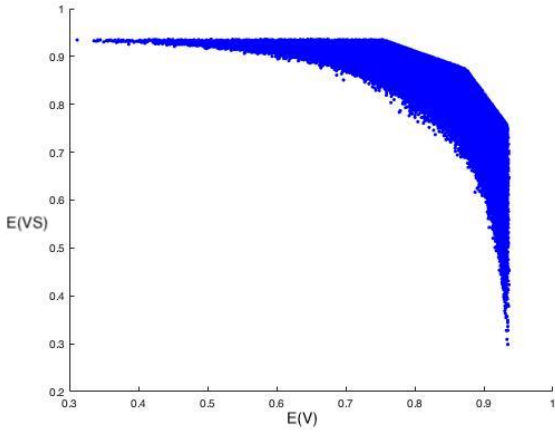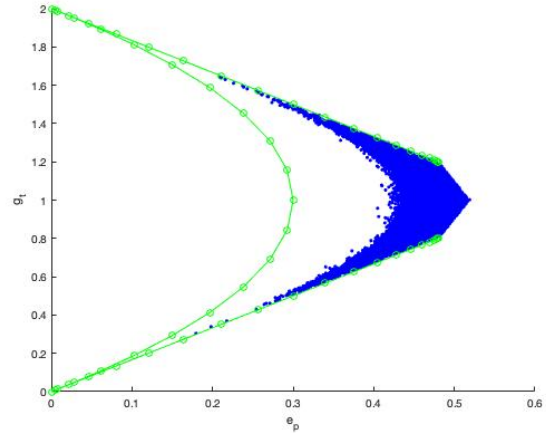(a) E(VS) vs E(V)   (b) $g_t(V)$ vs $e_p(V)$

Figure 4.1: Phase space plots for $V = (\mathbb{1} \otimes U \otimes \mathbb{1}) * (Ua \otimes Ub) * (\mathbb{1} \otimes U \otimes \mathbb{1})$ where U is a random unitary

In fig 4.1 b, the green lines are the boundary curves corresponding to the gates that form the 2 qubit boundary. It is clearly seen that the phase space is 'spilling' outside the right boundary (which is the $e_p - g_t$ curve for $(CNOT)S^\alpha$ family). This agrees with the fact that $(CNOT)S^\alpha$ does not form the right boundary in the 4 qubit case, which we have shown in chapter 3. To figure out the actual right boundary, we need to do some anaytical work, which is as of now, beyond the scope of this project. Hence, from now on, we will not show the right boundary in any plots.
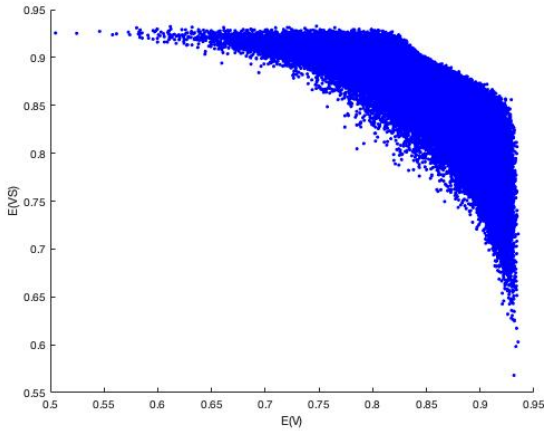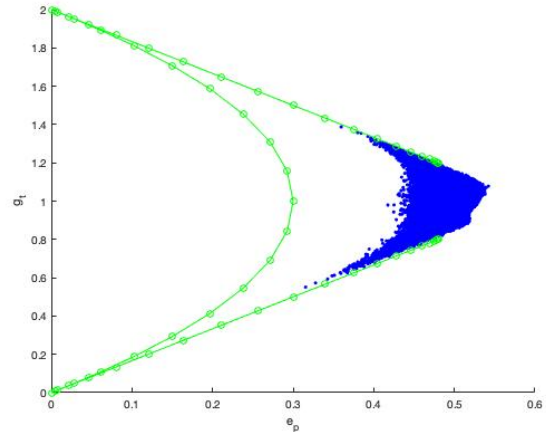
When U = CNOT gate :

(a) E(VS) vs E(V)

(b) $g_t(V)$ vs $e_p(V)$

Figure 4.2: Phase space plots for $V = (\mathbb{1} \otimes U \otimes \mathbb{1}) * (Ua \otimes Ub) * (\mathbb{1} \otimes U \otimes \mathbb{1})$ where U= CNOT

When $U = \sqrt{CNOT}$:

(a) E(VS) vs E(V)

(b) $g_t(V)$ vs $e_p(V)$

Figure 4.3: Phase space plots for $V = (\mathbb{1} \otimes U \otimes \mathbb{1}) * (Ua \otimes Ub) * (\mathbb{1} \otimes U \otimes \mathbb{1})$ where $U = \sqrt{CNOT}$

*

When U= Swap:

(a) E(VS) vs E(V)

(b) $g_t(V)$ vs $e_p(V)$

Figure 4.4: Phase space plots for $V = (\mathbb{1} \otimes U \otimes \mathbb{1}) * (Ua \otimes Ub) * (\mathbb{1} \otimes U \otimes \mathbb{1})$ where U=Swap

When $U = \sqrt{CNOT} * SWAP$:

(a) E(VS) vs E(V)

(b) $g_t(V)$ vs $e_p(V)$

Figure 4.5: Phase space plots for $V = (\mathbb{1} \otimes U \otimes \mathbb{1}) * (Ua \otimes Ub) * (\mathbb{1} \otimes U \otimes \mathbb{1})$ where $U = \sqrt{CNOT} * SWAP$

4.1.2 Case 2

$$V = (\mathbb{1} \otimes U \otimes \mathbb{1}) * (Ua1 \otimes Ua2 \otimes Ub1 \otimes Ub2) * (\mathbb{1} \otimes U \otimes \mathbb{1})$$

where U is 4*4 unitary, $\mathbb{1}$ is the 2*2 identity, Ua1, Ua2, Ub1 and Ub2 are 2*2 local unitaries.
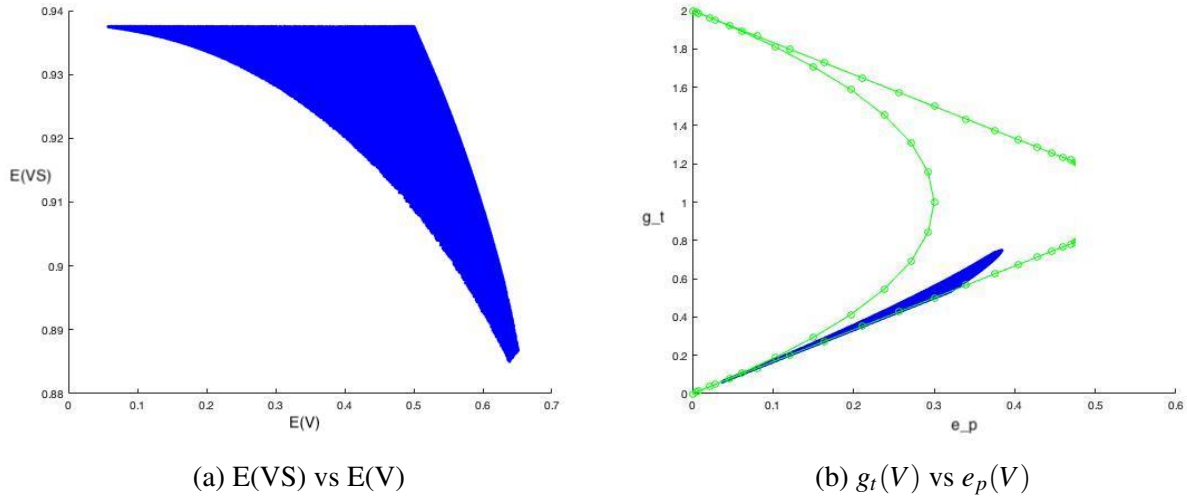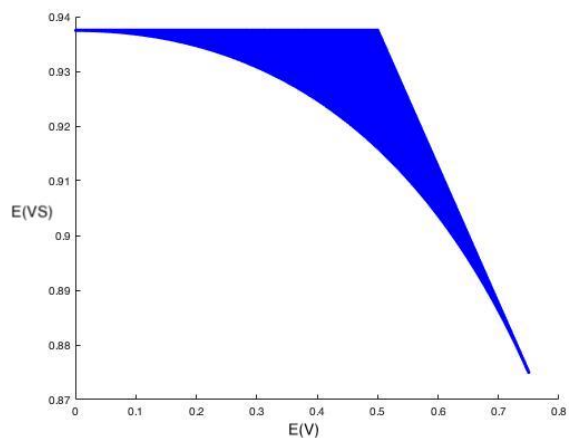
When U is a Haar random unitary :
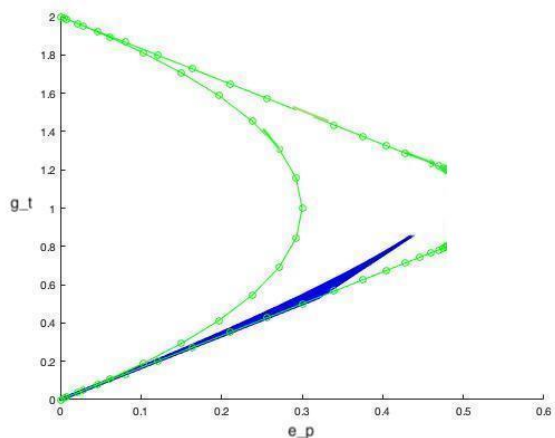

(a) E(VS) vs E(V) (b) $g_t(V)$ vs $e_p(V)$

Figure 4.6: Phase space plots for $V = (\mathbb{1} \otimes U \otimes \mathbb{1}) * (Ua1 \otimes Ua2 \otimes Ub1 \otimes Ub2) * (\mathbb{1} \otimes U \otimes \mathbb{1})$ where U is a random unitary

Here we can see that, in the case where U is a haar random unitary, when we use 4 single qubit gates instead of 2 bipartites (compare the first set of diagrams in Cases 1 and 2) it covers lesser area of the phase space. But such a difference is not observed when U is CNOT. It is interesting to note that the difference in the area covered is caused not just due to the non-local gates. The combination of local gates also affects the phase space drastically. It is interesting that even though local dynamics alone cannot affect the entangling power in any way, when interlaced between non-local gates, they affect the e_p dynamics of the significantly. *
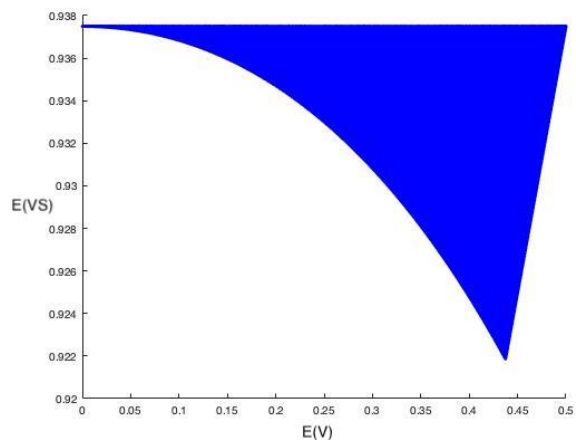
When U = CNOT :
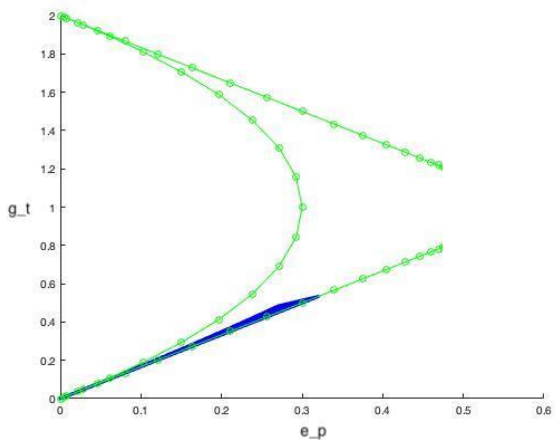

(a) E(VS) vs E(V)

(b) $g_t(V)$ vs $e_p(V)$

Figure 4.7: Phase space plots for $V = (\mathbb{1} \otimes U \otimes \mathbb{1}) * (Ua1 \otimes Ua2 \otimes Ub1 \otimes Ub2) * (\mathbb{1} \otimes U \otimes \mathbb{1})$ where U is CNOT

*

When $U = \sqrt{CNOT}$:

(a) E(VS) vs E(V)

(b) $g_t(V)$ vs $e_p(V)$

Figure 4.8: Phase space plots for $V = (\mathbb{1} \otimes U \otimes \mathbb{1}) * (Ua1 \otimes Ua2 \otimes Ub1 \otimes Ub2) * (\mathbb{1} \otimes U \otimes \mathbb{1})$ where $U = \sqrt{CNOT}$

4.1.3 Case 3

$$V = (U1 \otimes U \otimes U2) * (Ua \otimes Ub) * (U1 \otimes U \otimes U2)$$

where U is 4*4 unitary, U1 and U2 are 2*2 local unitaries, and Ua and Ub are 4*4 bipartites.

When U, U1 and U2 are fixed Haar random unitaries :

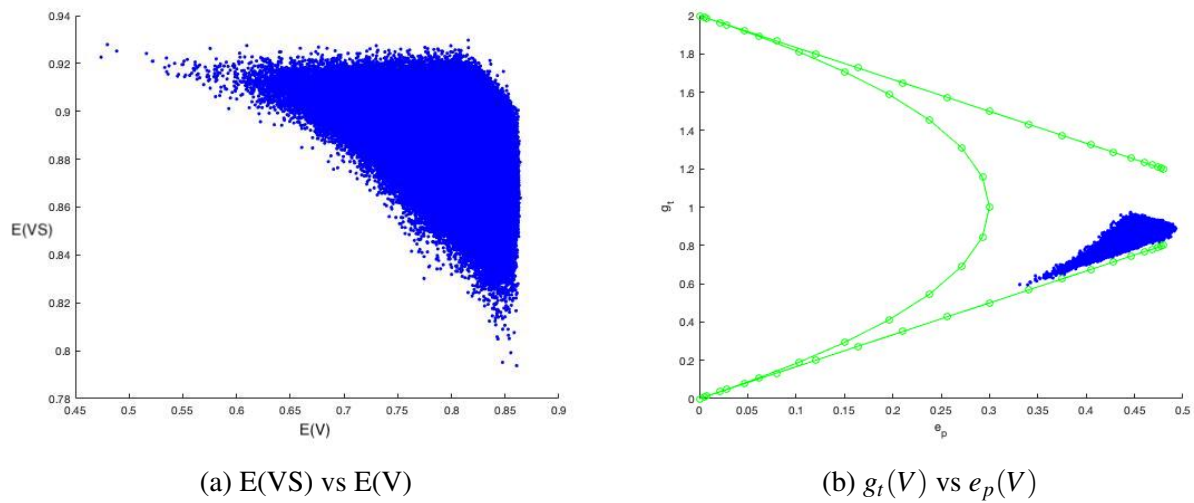(a) E(VS) vs E(V)   (b) $g_t(V)$ vs $e_p(V)$

Figure 4.9: Phase space plots for $V = (U1 \otimes U \otimes U2) * (Ua \otimes Ub) * (U1 \otimes U \otimes U2)$ where U is a random unitary

*

When U = CNOT and U1 & U2 are fixed haar random unitaries :

(a) E(VS) vs E(V)

(b) $g_t(V)$ vs $e_p(V)$
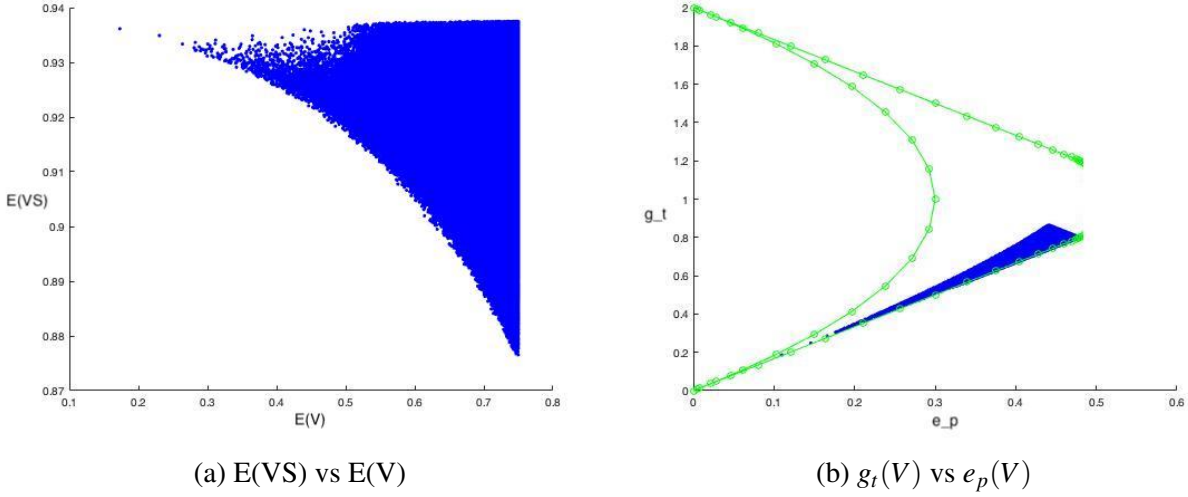
Figure 4.10: Phase space plots for $V = (U1 \otimes U \otimes U2) * (Ua \otimes Ub) * (U1 \otimes U \otimes U2)$ where U is CNOT

4.1.4 Case 4

$$V = (U1 \otimes U \otimes U2) * (Ua1 \otimes Ua2 \otimes Ub1 \otimes Ub2) * (U1 \otimes U \otimes U2)$$

where U is 4*4 unitary, U1 & U2 and Ua1, Ua2, Ub1 and Ub2 are 2*2 local unitaries.

Here we compare two cases : one where U is a haar random unitary and another where U is the CNOT gate. In both the cases, U1 and U2 are two unitaries randomly chosen according to haar measure, but fixed. We observe that more area of the phase space gets covered when U is a random unitary than when U is CNOT. This can be understood from the fact that $U = CNOT$ is just one special case and hence, this will cover an area of phase space that is a subset of the phase space when U is a haar random operator. It should be noted that this trend can be observed in other cases (with other combinations of gates) as well (for example, see case 3).
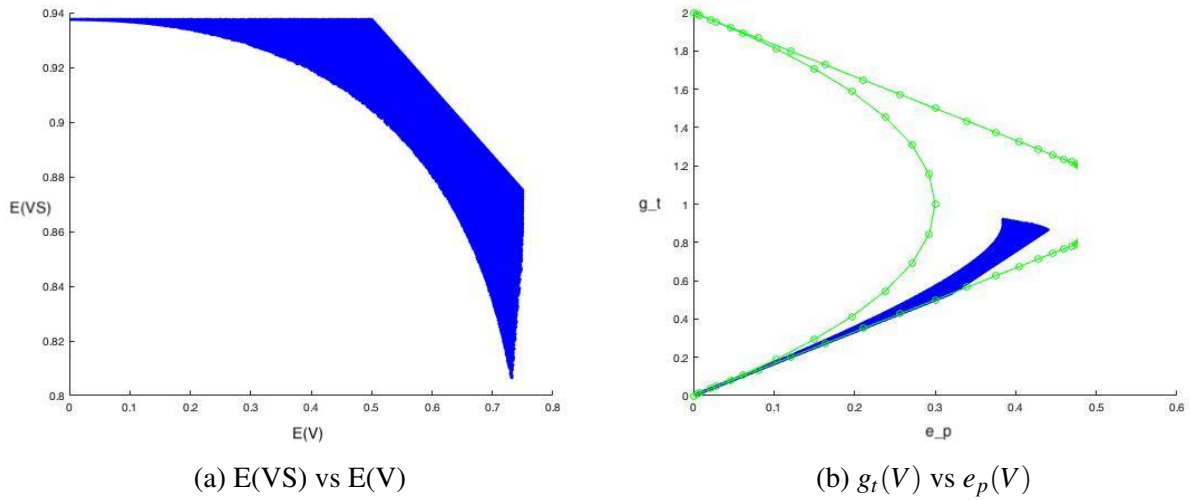
When U, U1 and U2 are fixed Haar random unitaries :

(a) E(VS) vs E(V)

(b) $g_t(V)$ vs $e_p(V)$

Figure 4.11: Phase space plots for $V = (U1 \otimes U \otimes U2) * (Ua1 \otimes Ua2 \otimes Ub1 \otimes Ub2) * (U1 \otimes U \otimes U2)$ where U is a random unitary

When U = CNOT and U1 & U2 are fixed haar random unitaries :
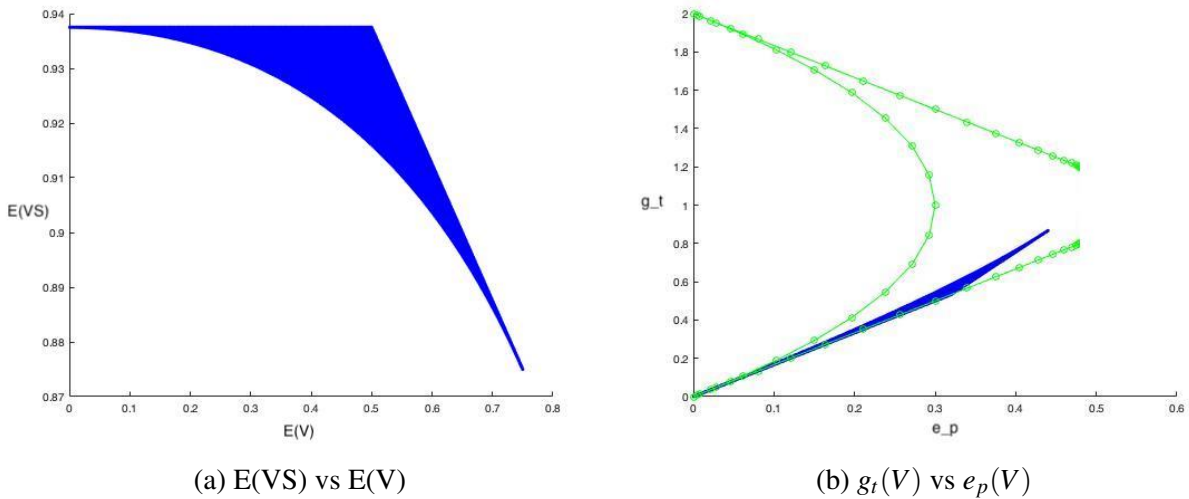

(a) E(VS) vs E(V)

(b) $g_t(V)$ vs $e_p(V)$

Figure 4.12: Phase space plots for $V = (U1 \otimes U \otimes U2) * (Ua1 \otimes Ua2 \otimes Ub1 \otimes Ub2) * (U1 \otimes U \otimes U2)$ where U is CNOT

35

4.2 When the non-local operator is $U_{16\times 16}$

4.2.1 Case 1

$$V = U * (I \otimes Ua \otimes Ub \otimes I) * U$$

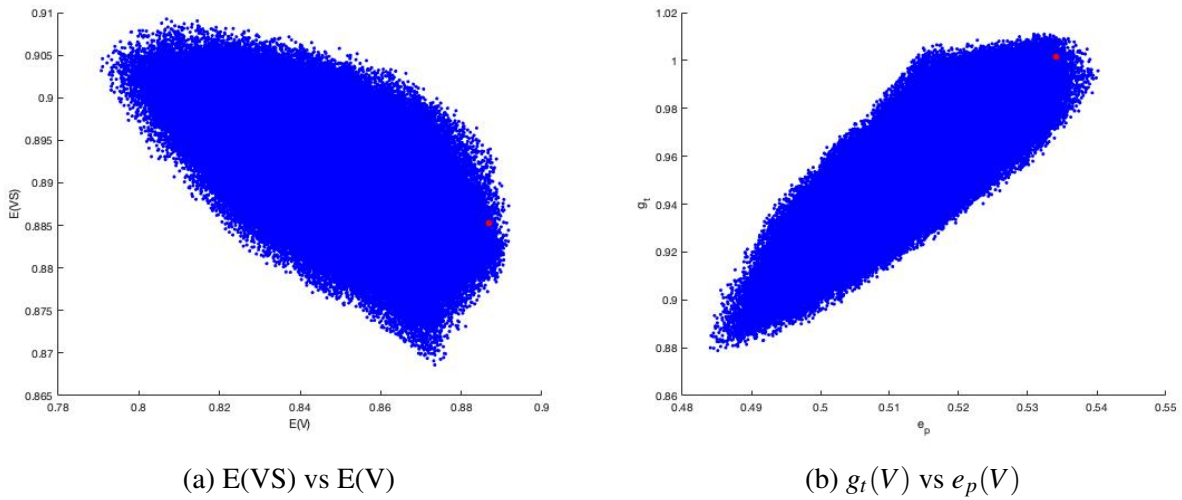where U is a 16*16 random unitary, Ua and Ub are Haar random 2*2 unitaries and I is the 2*2 Identity.

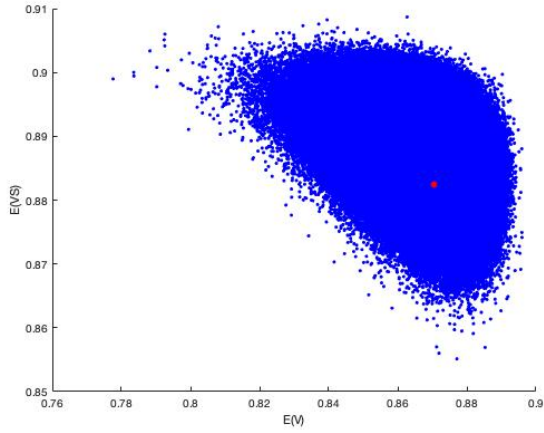(a) E(VS) vs E(V)　　　　　　　(b) $g_t(V)$ vs $e_p(V)$

Figure 4.13: Phase space plots for $V = U * (I \otimes Ua \otimes Ub \otimes I) * U$ where U is a random unitary
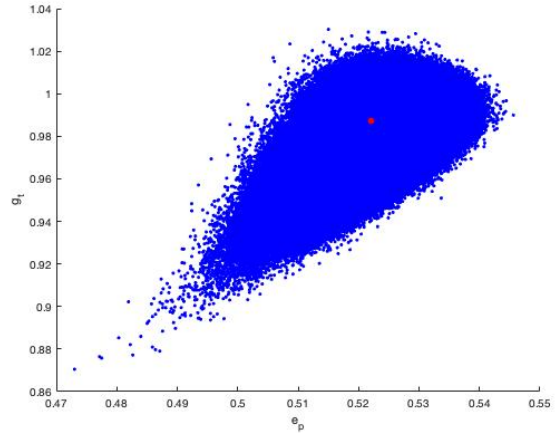
*

4.2.2 Case 2

$$V = U * (Ua1 \otimes Ua2 \otimes Ub1 \otimes Ub2) * U$$

Here Ua1, Ua2, Ub1, Ub2 are 2*2 local Haar random operators.

36

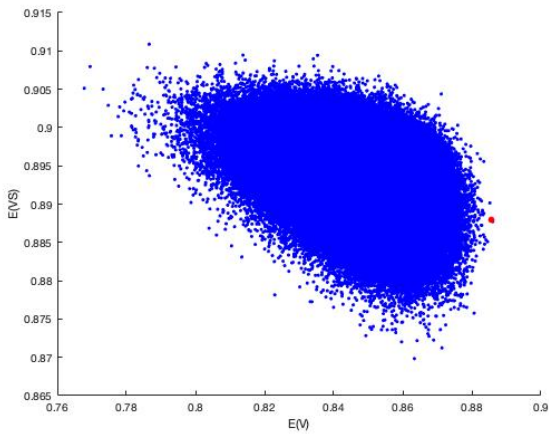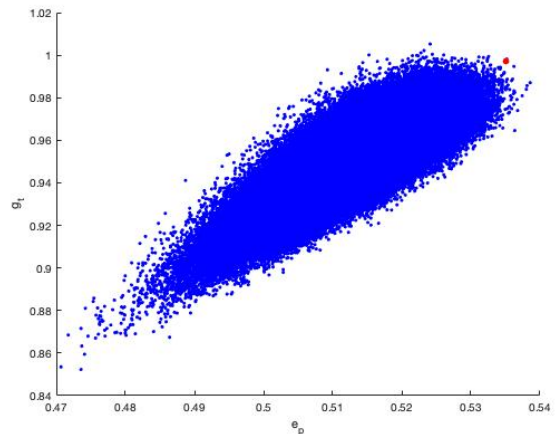(a) E(VS) vs E(V)　　　　　　　　　　(b) $g_t(V)$ vs $e_p(V)$

Figure 4.14: Phase space plots for $V = U * (Ua1 \otimes Ua2 \otimes Ub1 \otimes Ub2) * U$ where U is a random unitary

4.2.3　Case 3

$V = U * (Ua \otimes Ub) * U$ where Ua and Ub are 4*4 unitaries.

(a) E(VS) vs E(V)　　　　　　　　　　(b) $g_t(V)$ vs $e_p(V)$

Figure 4.15: Phase space plots for $V = U * (Ua \otimes Ub) * U$ where U is a random unitary
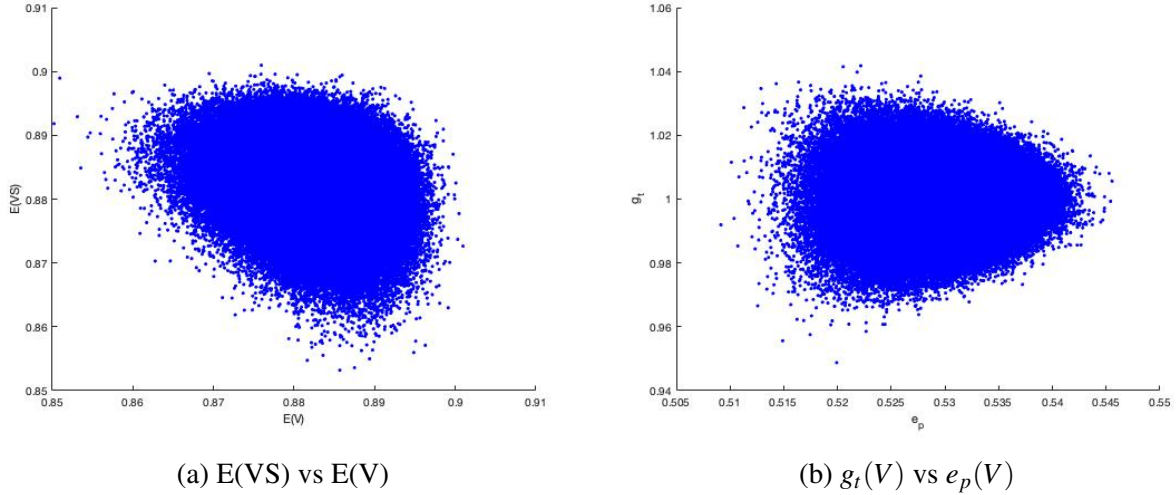
37

4.2.4 Case 4

$V = U$ (only 16*16 by unitaries)

(a) E(VS) vs E(V) (b) $g_t(V)$ vs $e_p(V)$

Figure 4.16: Phase space plots for 16×16 random unitaries

Here it should be noted that when we interlace locals between two operations of a 16*16 haar random unitary, the phase space expands, i.e operator entanglement is enhanced. We can observe that in cases 1, 2 and 3 the area of phase space covered is almost the same but compared to the phase space of only 16*16 unitaries (case 4), these cover significantly larger area of the phase space. Hence we can conclude that our simulations for the 4 qubit case agree with the theory in [7].

4.3 Trajectory approach

To plot the phase space diagrams of 16*16 unitaries (without any locals), we start with U=S and in each iteration some power of S (the 4 qubit Swap operator) and some power of CNOT is multiplied with the 'U' from the previous iteration and then the e_p and g_t values are calculated. The powers to which S and CNOT are raised, were chosen randomly and are changed after every 20000 (tentatively) iterations.The same is repeated starting from U=$\mathbb{1}$. This gives us many trajectories, all of which when put together seem to cover the entire phase space. We choose S and $\mathbb{1}$ as starting

points because we know that these operators take the extreme (max/min) values for e_p and g_t and hence will definitely lie on an end point of the phase space.

A sample algorithm for this method would be as follows:

- We start with say $U = S$

- For the first set of iterations, $U = \sqrt{S} * \sqrt{CNOT} * U$

- For the next set, $U = S^{0.2} * CNOT^{0.7} * U$

- And then $U = S^{0.4} * CNOT^{0.6} * U$

- and so on

Again the same algorithm is repeated starting from U=$\mathbb{1}$. From section 3.3, recall that for the 4 qubit case, it is possible to construct a permutation matrix P which has the maximum e_p value. So, it is clear that P will be one end point of the phase space. Hence, it will be useful to repeat the above algorithm and plot a trajectory starting from P as well. When we put all the trajectories (starting from S, $\mathbb{1}$ and P) together, we obtain the full phase space (fig 4.17).

(a) E(US) vs E(U)   (b) $g_t(U)$ vs $e_p(U)$
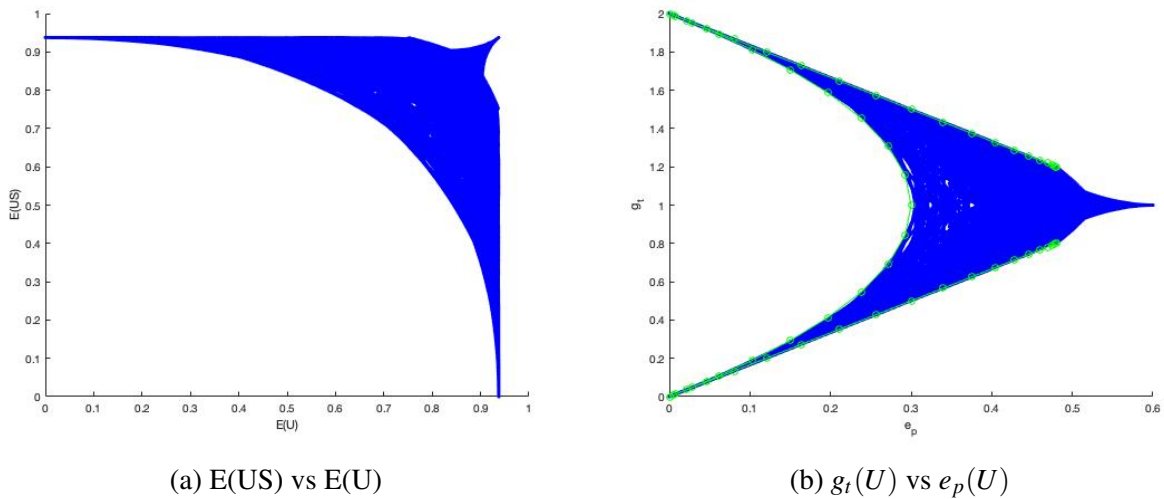
Figure 4.17: Total phase space for N=4; plotted using the trajectory approach

The drawback with this method is that the trajectories are all deterministic and there is no random sampling.
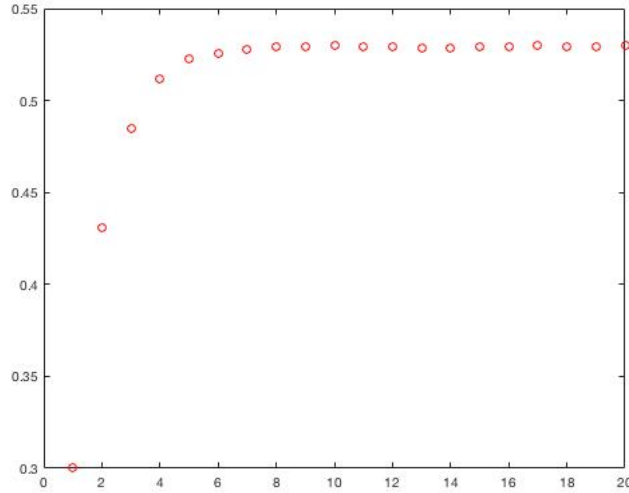
4.4 e_p vs n

Figure 4.18: e_p vs the number of iterations

As in the 2 qubit case [7], we can plot e_p averaged over local gates vs the number of iterations of U interlaced with local gates. Here we consider the operator

$$V = U \ (U_A^1 \otimes U_B^1) \ U \ (U_A^2 \otimes U_B^2) \ U........U \ (U_A^n \otimes U_B^n) \ U \tag{4.1}$$

where U is a $16 * 16$ unitary and U_A^i and U_B^i are $4 * 4$ local gates. n is the number of iterations. For each n, an ensemble average of e_p is calculated. It is seen that it converges exponentially (fig 4.18) to the mean e_p value given by

$$\bar{e_p} = \frac{(N-1)^2}{(N^2+1)} = \frac{9}{17} = 0.529 \tag{4.2}$$

Similar behaviour is seen in gate typicality as well. This shows that the two quantities entangling power and gate typicality are modified significantly by subsequent application of local gates [7].

Chapter 5

Conclusion

In this work we have studied the ensemble of iterated unitary quantum gates distributed uniformly with respect to the Haar measure on the unitary group. To begin with, we highlighted the definition of operator entanglement using the connection between the operator Schmidt coefficients of an operator U and the normalized squared singular values of the reshuffled matrix U_R [7]. We then studied the effect of interlacing haar random local gates in the 2 qubit case [7] and extended this to the 4 qubit system.

The first part of our study of the 4 qubit system was understanding the boundaries. We derived the equation for S^α and $(CNOT)S^\alpha$ parabolas and showed that $(CNOT)S^\alpha$ cannot form the right boundary. We also derived the upper and lower bounds on g_t and showed that these boundaries are the $e_p - g_t$ curves for $S(CNOT)^\alpha$ and $(CNOT)^\alpha$. We could also identify two permutation matrices with maximum and minimum e_p using the method described in [11]. We can now make use of the permutation matrix to derive the right boundary of the phase space.

In the second part, we plotted the phase space diagrams for different combinations of local gates. This helped in understanding the how local dynamics affects the entangling power and gate typicality. We could compare the two cases : 1) when the local part is four single qubit random unitaries i.e $U^{A1} \otimes U^{A2} \otimes U^{B1} \otimes U^{B2}$ and 2) when the local part is two bipartite random unitaries i.e $U^A \otimes U^B$. We also tried out different forms of non-local operators and saw how the phase space changes with different operators like CNOT, Swap, $\sqrt{CNOT}$ etc. By analyzing the effect of local dynamics, we concluded that our simulations for the 4 qubit system agree with the theory in [7], i.e

interlacing random local gates (whatever combination it may be) between fixed non-local operators indeed enhances the operator entanglement.

Future prospective

The broad aim of this project was to extend the work in [7] to higher dimensional systems i.e study the entanglement properties of haar random quantum operators in systems with $N \geq 3$. In this work, we have briefly looked at the $N = 4$ case. The next step would be to analytically solve for the left and right boundaries of the 4 qubit phase spece. Then it will be interesting to look at other dimensions. One possible direction is to study the difference in dynamics of odd-dimensional and even-dimensional systems, if any. We can also take up $N = 6$ as a special case of study as it is the only case (other than $N = 2$) where we cannot construct a permutation matrix with maximum e_p [11]. Then if possible, we will analytically study the boundaries of higher dimensional phase spaces and look for a pattern.

Appendix A

Haar measure

In quantum mechanics, evolution of a state vector $\psi(t)$ is described by a unitary transformation.

$$\psi(t) = U\psi(0) \tag{A.1}$$

Being unitary, U preserves the inner product and guarantees $||\psi(t)|| = ||\psi(0)||$ which is required by probabilistic interpretations of quantum mechanics. Hence, U plays an important role in solving for the dynamics of a quantum mechanical system. But, in case the system is complicated, one can attempt to solve by replacing U with a random unitary operator. But for defining a random unitary operator we need atleast a measure on the matrix space and it turns out to be Haar measure.

Definition

In general, consider a group G and a measure μ on G, then $\forall g \in G$,

$$\int_G f(x)\, d\mu(x) = \int_G f(gx)\, d\mu(x) \tag{A.2}$$

where the non-zero measure $\mu : G \to [0, \infty]$ is such that for all $S \subseteq G$ and $g \in G$,

$$\mu(gS) = \mu(Sg) = \mu(S) \tag{A.3}$$

where

$$\mu(S) := \int_{g \in S} d\mu(g) \tag{A.4}$$

Here, μ is called the *Haar measure*. It is defined on every compact topological group and is unique If $\mu(G) = 1$, then it is called a probability measure. [12]

The columns (or rows) of a unitary matrix form an orthonormal basis in $\mathbb{C}^N$. The set $U(N)$ of unitary matrices forms a compact Lie group whose real dimension is N^2. It is then made into a probability space by assigning as a distribution, the unique measure invariant under group multiplication known as *Haar measure*. Such a probability space is often referred to as *Circular Unitary ensemble* (CUE).

Haar measure normalized to one is a natural choice for a probability measure on a compact group because being invariant under group multiplication, any region of $U(N)$ carries the same weight in a group average. It is the analogue of the *uniform density* on a finite interval. Also, if the system does not have any symmetry, then there are no restrictions on $U(N)$ and the natural choice of probability distribution is Haar measure.

Example : haar measure on $U(1)$

Consider $U(1)$. It is the set $\{e^{i\theta}\}$ of complex numbers with modulo 1 and it has the topology of the unit circle $\mathbb{S}^1$. Since in this case, matrix multiplication is simply addition mod 2π, $U(1)$ is isomorphic to the group of translations on $\mathbb{S}^1$. A probability density function that equally weighs any part of the unit circle is the constant density $\rho(\theta) = \dfrac{1}{2\pi}$. This is invariant under translations and hence, it is the unique haar measure on $U(1)$.

Algorithm

An algorithm to choose random unitary marices $U(N)$ according to haar measure has been given by Mezzadri. [13] This algorithm is based on QR decomposition and for this entire project work, we have made use of this algorithm to choose haar random unitaries. The algorithm is as follows:

- Take an $N \times N$ complex matrix Z whose entries are complex standard normal random variables.

- Input Z into any QR decomposition routine. Let (Q, R), where $Z = QR$, be the output.

- Create the following **diagonal** matrix

$$\Lambda = \begin{pmatrix} \dfrac{r_{11}}{|r_{11}|} & .. & .. & .. \\ .. & .. & .. & .. \\ .. & .. & .. & .. \\ .. & .. & .. & \dfrac{r_{NN}}{|r_{NN}|} \end{pmatrix} \qquad (A.5)$$

  where the r_{jj}s are the diagonal elements of R.

- The diagonal elements $R' = \Lambda^{-1}R$ are always real and strictly positive. Therefore, the matrix $Q' = Q\Lambda$ is distributed with Haar measure.

Appendix B

Distribution of e_p and g_t

As we saw in Chapter 4, when we use the function based on the above algorithm to choose haar random unitaries, the unitaries do not span the full expected phase space for higher N values. For $N = 2$, if we look at the $E(VS)$ vs $E(V)$ or g_t vs e_p plots, the entire phase space seems to be getting filled. But for N=4, we have noticed that the unitaries seem to be concentrated only around a small region around the mean values (averaged over the Haar measure) given by

$$\bar{e}_p = \frac{(N-1)^2}{(N^2+1)} \tag{B.1}$$

and

$$\bar{g}_t = 1 \tag{B.2}$$

Hence in order to confirm this, it will be useful to look at the probability distribution of e_p and g_t for different dimensions. Here, we will look at the probability distribution of e_p and g_t for $N = 2, 4$ and 6.

After plotting the distribution curves and comparing them (fig B.4 - see [8]), it is clear that as N increases, those unitaries are preferentially chosen whose e_p and g_t values are close to the above mentioned average values. From fig B.4, we can see that the distribution gets narrower as N increases.
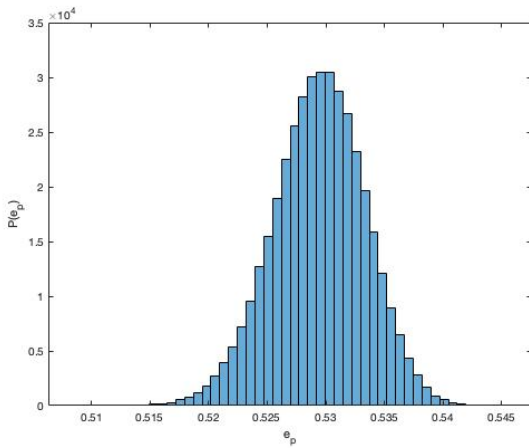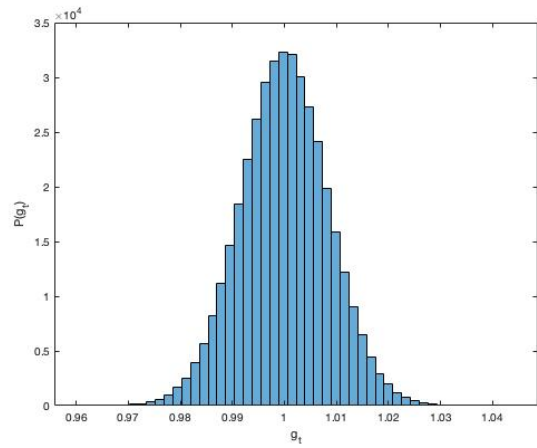
N=2
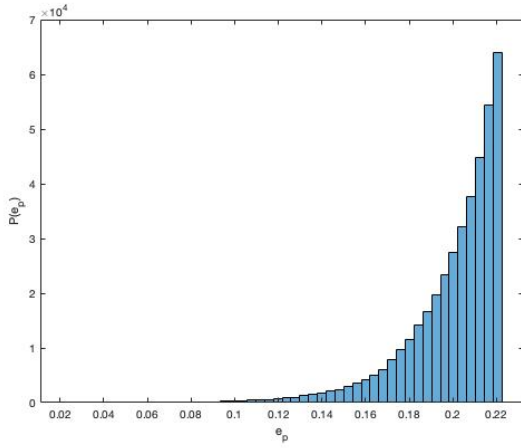
(a) Distribution of e_p
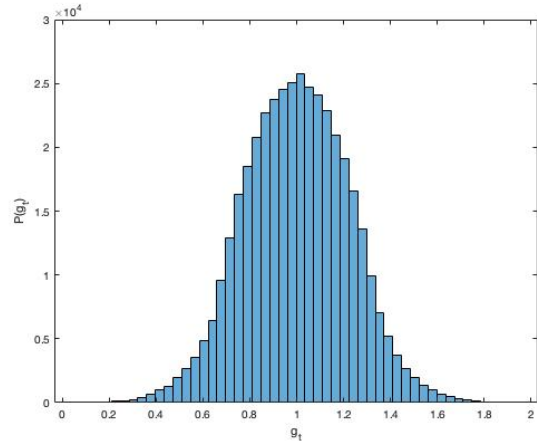
(b) Distribution of g_t

Figure B.1: Distribution of probability density of e_p and g_t for $N = 2$
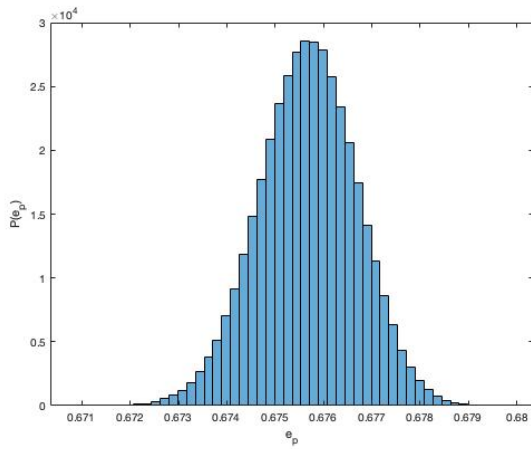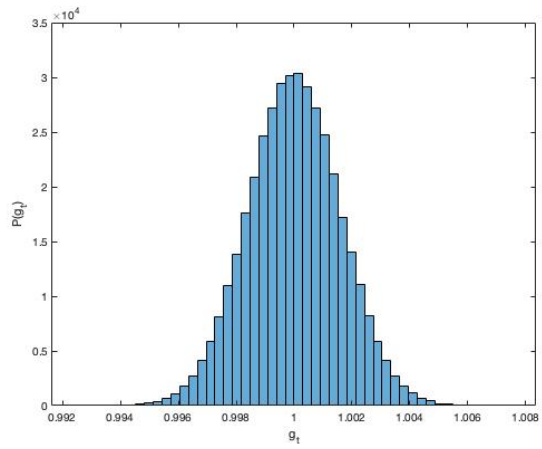
N=4

(a) Distribution of e_p

(b) Distribution of g_t

Figure B.2: Distribution of probability density of e_p and g_t for $N = 4$

N=6

(a) Distribution of e_p

(b) Distribution of g_t

Figure B.3: Distribution of probability density of e_p and g_t for $N = 6$
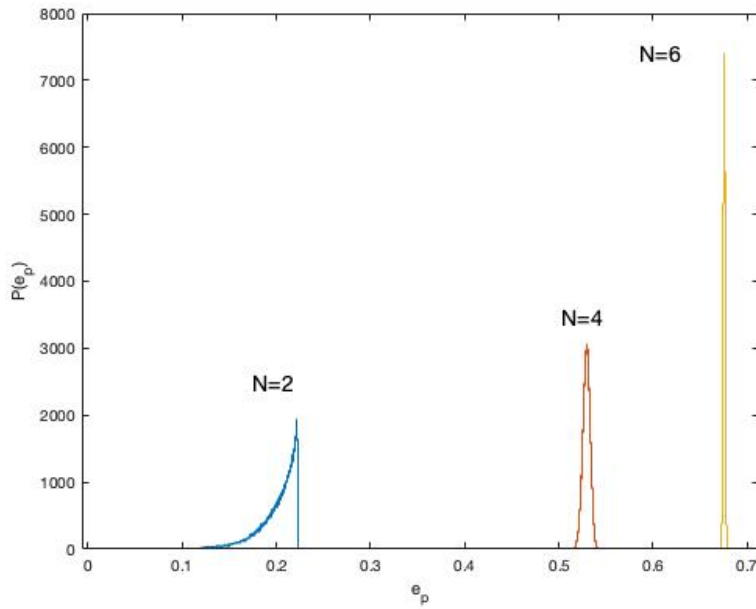

Figure B.4: Comparing the distributions of probability density of e_p for $N = 2, 4$ and 6

Appendix C

Phase space diagrams for N= 6 using trajectory approach
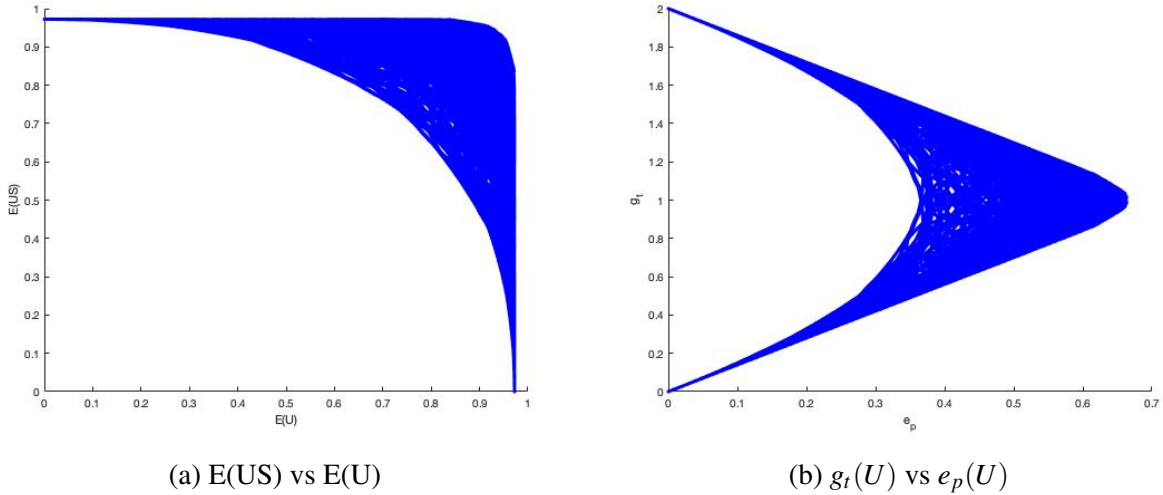

(a) E(US) vs E(U)

(b) $g_t(U)$ vs $e_p(U)$

Figure C.1: Phase space plots for N=6 using trajectory method

Here, we have plotted the phase spae diagrams for $N = 6$ using the trajectory approach, taking $\mathbb{1}$ ans Swap as the starting points. $N = 6$ is an interesting system to study as it is the case (other than $N = 2$) where we cannot construct a permutation matrix with maximum e_p [11]. We also know that higher dimensional generalization of CNOT is not a maximal operator [8]. Hence, it would be interesting to look at what kind of gates can form the right boundary for the $e_p - g_t$ phase space.

Bibliography

[1] Michael A Nielsen and Isaac L Chuang. Quantum computation and quantum information. Cambridge university press, 2010.

[2] Adam Nahum, Sagar Vijay, and Jeongwan Haah. Operator Spreading in Random Unitary Circuits, Phys. Rev. X 8, 021014 – April 2018

[3] R. Oliveira, O. C. O. Dahlsten, and M. B. Plenio. Generic Entanglement Can Be Generated Efficiently, Phys. Rev. Lett. 98, 130502 – March 2007

[4] Fernando G. S. L. Brandão, Aram W. Harrow, Michał Horodecki. Local Random Quantum Circuits are Approximate Polynomial-Designs, Communications in Mathematical Physics, 2016, Volume 346, Number 2, Page 397

[5] Michael A Nielsen, Christopher M Dawson, Jennifer L Dodd, Alexei Gilchrist, Duncan Mortimer, Tobias J Osborne, Michael J Bremner, Aram W Harrow, and Andrew Hines. Quantum dynamics as a physical resource. Physical Review A, 67(5):052301, 2003.

[6] Karol Zyczkowski, Ingemar Bengtsson. On Duality between Quantum Maps and Quantum States, Open Systems & Information Dynamics, 2004, Volume 11, Number 1, Page 3

[7] Bhargavi Jonnadula, Prabha Mandayam, Karol Życzkowski, and Arul Lakshminarayan. Impact of local dynamics on entangling power, Phys. Rev. A 95, 040302(R) – April 2017

[8] Paolo Zanardi, Christof Zalka, and Lara Faoro. Entangling power of quantum evolutions. Phys. Rev. A 62, 030301(R) – August 2000

[9] Juan Carlos Garcia-Escartin, Pedro Chamorro-Posada, A SWAP gate for qudits, Quantum Information Processing, 2013, Volume 12, Number 12, Page 3625

[10] H. A. Sa Earp and J. K. Pachos, A constructive algorithm for the Cartan decomposition of $SU(2^N)$ J. Math. Phys.46, 1(2005)

[11] Lieven Clarisse, Sibasish Ghosh, Simone Severini, Anthony Sudbery, Entangling Power of Permutations, 2005, Physical Review A 72(1)

[12] Simon Rubinstein-Salzedo. On the existence and uniqueness of invariant measures on locally compact groups. Math. Notes, 2004.

[13] Francesco Mezzadri. How to generate random matrices from the classical compact groups. arXiv preprint math-ph/0609050, 2006.

[14] Bhargavi Jonnadula, Prabha Mandayam, Karol Życzkowski, and Arul Lakshminarayan. Operator entanglement and the effect of local dynamics. *"in preparation"*

[15] Po-Yao Chang, Xiao Chen, Sarang Gopalakrishnan, J. H. Pixley. Evolution of entanglement spectra under random unitary dynamics. arXiv preprint 1811.00029v2, 2018

[16] Bhargavi Jonnadula. Effect of local unitaries on iterated nonlocal unitaries. BS-MS thesis, IIT Madras, April 2016.

[17] Arul Lakshminarayan, Zbigniew Puchała, and Karol Życzkowski. Diagonal unitary entangling gates and contradiagonal quantum states. Phys. Rev. A 90, 032303, 2014.

[18] Yi Shen and Lin Chen. Entangling power of two-qubit unitary operations. Journal of Physics A: Mathematical and Theoretical, Volume 51, Number 39, 2018